

**CFD-BASED ANALYSIS AND OPTIMIZATION OF  
WIND BOOSTERS FOR LOW SPEED VERTICAL AXIS  
WIND TURBINES**

**BY**

**NATAPOL KORPRASERTSAK**

**A THESIS SUBMITTED IN PARTIAL FULFILLMENT OF THE  
REQUIREMENTS FOR THE DEGREE OF MASTER OF SCIENCE  
(ENGINEERING AND TECHNOLOGY)  
SIRINDHORN INTERNATIONAL INSTITUTE OF TECHNOLOGY  
THAMMASAT UNIVERSITY  
ACADEMIC YEAR 2015**

**CFD-BASED ANALYSIS AND OPTIMIZATION OF  
WIND BOOSTERS FOR LOW SPEED VERTICAL AXIS  
WIND TURBINES**

**BY**

**NATAPOL KORPRASERTSAK**

**A THESIS SUBMITTED IN PARTIAL FULFILLMENT OF THE  
REQUIREMENTS FOR THE DEGREE OF MASTER OF SCIENCE  
(ENGINEERING AND TECHNOLOGY)  
SIRINDHORN INTERNATIONAL INSTITUTE OF TECHNOLOGY  
THAMMASAT UNIVERSITY  
ACADEMIC YEAR 2015**



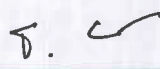
CFD-BASED ANALYSIS AND OPTIMIZATION OF WIND BOOSTERS FOR  
LOW SPEED VERTICAL AXIS WIND TURBINES

A Thesis Presented

By  
NATAPOL KORPRASERTSAK

Submitted to  
Sirindhorn International Institute of Technology  
Thammasat University  
In partial fulfillment of the requirements for the degree of  
MASTER OF SCIENCE (ENGINEERING AND TECHNOLOGY)

Approved as to style and content by

Advisor and Chairperson of Thesis Committee   
(Prof. Thananchai Leephakpreeda, Ph.D.)

Committee Member   
(Assoc. Prof. Supachart Chungpaibulpatana, D.Eng)

Committee Member and Chairperson  
of Examination Committee   
(Asst. Prof. Anotai Suksangpanomrung, Ph.D.)

APRIL 2015

## **Abstract**

### **CFD-BASED ANALYSIS AND OPTIMIZATION OF WIND BOOSTERS FOR LOW SPEED VERTICAL AXIS WIND TURBINES**

By

NATAPOL KORPRASERTSAK

Mechanical Engineering: Sirindhorn International Institute of Technology, 2012

Although Vertical Axis Wind Turbines (VAWTs) are designed for performing mechanical works acceptably at medium wind speed, Standalone VAWTs are still unable to generate mechanical power satisfactorily for best practice at low speed wind. This study presents analysis and optimal design of wind booster, by utilizing Computational Fluid Dynamics (CFD). A wind booster is proposed to be implemented with a VAWT in order to not only harvest energy with low availability at low wind speed but also enhance performance of a VAWT at higher wind speed. In CFD-based experiments, guiding and throttling effects of the wind booster are able to increase mechanical power of a VAWT. Optimal alternatives of number, shape, and leading angle of guide vanes are determined by maximizing the coefficient of power from the alternating direction method as an optimization technique. The VAWT coupled with the optimal wind booster, which consists of 8 straight-line guide vanes and leading angle of  $76.1^\circ$ , is capable of producing mechanical power higher up to the coefficient of power of 5.56 % than the original design.

**Keywords:** Wind Booster, Vertical Axis Wind Turbine, Low Wind Speed, Computational Fluid Dynamics, Optimization

## **Acknowledgements**

The author would like to thank Bangchak Petroleum PCL for financial support under “The Bangchak Graduate Scholarship” program BC-SIIT-G-S1Y13/012, Sirindhorn International Institute of Technology for financial support, working office, some apparatuses and especially XFlow™ CFD software which was mainly used in big parts of the research, The SIIT mechanical technician, Mr. Nikhom Meedet, who helped to build the prototype of plastic wind turbine and the wind booster and also, helped to supply so many apparatuses, and finally, the author would like to give special thanks to the advisor supervising this research, Prof. Dr. Thananchai Leephakpreeda, who provided many important comments and suggestions making the research progress in the right direction until achieving the research’s goal.

## Table of Contents

Chapter	Title	Page
	Signature Page	i
	Abstract	ii
	Acknowledgement	iii
	Table of Contents	iv
	List of Tables	vi
	List of Figures	vii
1	Introduction	1
	1.1 Statement of problem	1
	1.2 Purpose of study	4
	1.3 Significance of study	4
2	Literature Review	5
	2.1 Vertical axis wind turbines	5
	2.2 Development of wind boosters	6
3	Methodology	9
	3.1 Modelling and design of wind boosters	10
	3.2 Power analysis on VAWTs	15
	3.3 CFD-based analysis on VAWTs and wind boosters	16
	3.4 Optimization algorithm	20
4	Results and Discussion	26

4.1 Performance analysis on VAWTs and VAWT with wind boosters	26
4.1.1 Mechanism of wind booster	27
4.1.2 VAWTs and wind boosters in no loading condition	28
4.1.3 VAWTs and wind boosters in various loading condition	34
4.2 Optimization of wind boosters	40
5 Conclusions and Recommendations	48
5.1 Conclusions	48
5.2 Recommendations	48
References	49
Appendices	51
Estimation of Peak Coefficient of Power	52
VAWT Angular speed VS time	53

## List of Tables

<b>Tables</b>	<b>Page</b>
3.1 Specification of the VAWT	12
3.2 Specification of the wind booster	13
3.3 Simulation setup	19
4.1 Angular Speeds of VAWT at various wind speeds	29
4.2 Torque and mechanical power against VAWT speed at various wind speed	34
4.3 Optimization for curved side triangle shape of guide vane	41
4.4 Optimization for straight side triangle shape of guide vane	41
4.5 Optimization for straight line shape of guide vane	42
4.6 Optimal design variables for the three different shapes of guide vanes	43
4.7 Optimization for straight line shape of guide vane with initial $\beta$ of 8	45



## List of Figures

<b>Figures</b>	<b>Page</b>
1.1 Wind resource assessment in Thailand	3
2.1 Wind booster	6
3.1 Schematic diagram of VAWT and wind booster	11
3.2 Leading angle of the preliminary wind booster	12
3.3 Dimension of the VAWT	13
3.4 Dimension of the wind booster	14
3.5 Assembly of the VAWT and the wind booster	14
3.6 VAWT exerted by external torques	17
3.7 XFlow <sup>TM</sup> CFD's user interface	18
3.8 Typical plots of coefficient of power against tip speed ratio	20
3.9 The wind booster with curved side triangle shape of guide vane	21
3.10 The wind booster with straight side triangle shape of guide vane	22
3.11 The wind booster with straight line shape of guide vane	22
3.12 Leading angle of guide vane	22
3.13 Alternating direction technique in CFD experiments	23
3.14 Algorithm of alternating direction technique	25
4.1 CFD simulation of VAWT without wind booster	27
4.2 CFD simulation of VAWT with wind booster	27
4.3 Wind flowing through VAWT with the wind booster	28
4.4 Plots of VAWT angular speed against wind speed	29
4.5 VAWT with wind booster during the experiment process	30
4.6 Plots of VAWT angular speed against wind speed (Experimental case)	31
4.7 Working three-cup anemometer in wind measurement	31
4.8 Input wind speed in CFD simulation	32
4.9 Plot of VAWT speed against time for 0.5 m/s of average wind input	33
4.10 Plot of VAWT speed against time for 3 m/s of average wind input	34
4.11 Plots of torques against VAWT angular speeds without wind booster	37
4.12 Plots of torques against VAWT angular speeds with wind booster	38

4.13 Plots of powers against VAWT angular speeds without wind booster	38
4.14 Plots of powers against VAWT angular speeds with wind booster	39
4.15 Plots of power coefficient against VAWT tip speed ratio	40
4.16 Plots of development of peak values of coefficient of power	44
4.17 The optimal wind booster	44
B.1 Plot of VAWT angular speed against time for wind speed of 1 m/s	53
B.2 Plot of VAWT angular speed against time for wind speed of 2 m/s	54
B.3 Plot of VAWT angular speed against time for wind speed of 3 m/s	54
B.4 Plot of VAWT angular speed against time for wind speed of 4 m/s	55
B.5 Plot of VAWT angular speed against time for wind speed of 5 m/s	55
B.6 Plot of VAWT angular speed against time for wind speed of 6 m/s	56
B.7 Plot of VAWT angular speed against time for wind speed of 7 m/s	56
B.8 Plot of VAWT angular speed against time for wind speed of 8 m/s	57

# Chapter 1

## Introduction

### 1.1 Statement of problem

No one can reject the fact that fossil fuel is gradually depleted nowadays because of overconsumption from humans and fossil fuel is not renewable energy, therefore it is impossible that fossil fuel can generate itself to satisfy humans' demand. As demand of fossil fuel is higher than supply, price of fossil fuel continuously increases. A way to solve this critical situation is to improve use of renewable energy. Renewable energy sources can be considered as free energy sources as this kind of energy does not deplete no matter how much it is consumed. As one of renewable energy, wind energy now becomes mainstream alternative energy from fossil-based energy (Walker, 2009). This requires a lot of improvement to achieve practical usage efficiently.

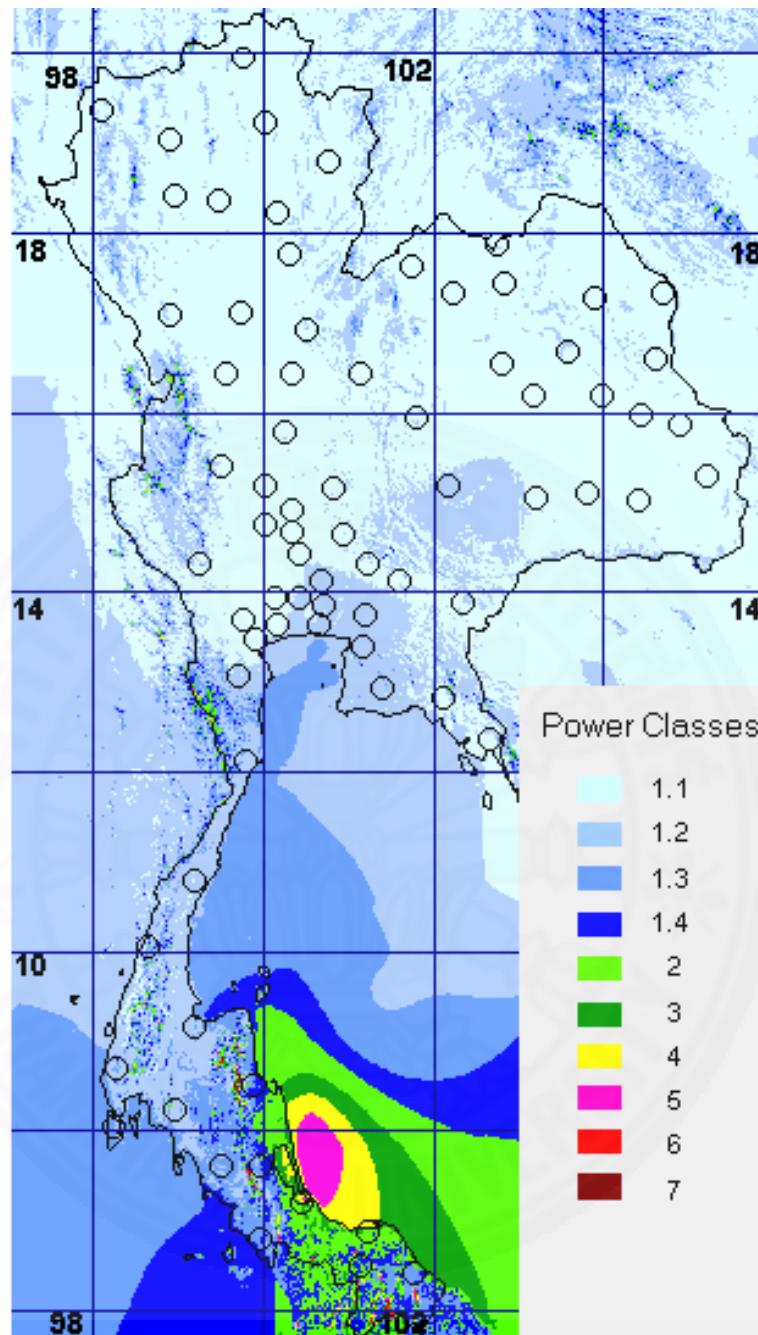
Nowadays, wind power generation systems mostly consist of Horizontal Axis Wind Turbines (HAWTs) in mid to large-scale wind farms since HAWTs perform mechanical works efficiently at high wind speeds. In many accessible areas of Thailand, the average wind speed is relatively low, approximately with 2-4 m/s at heights of 40 m. Therefore, Vertical Axis Wind Turbines (VAWTs) are chosen to be installed instead of HAWTs because VAWTs are designed to yield acceptable performances on mechanical works at medium wind speeds. However, standalone VAWTs do not sufficiently yield the most effective wind power conversion due to the limitation of harvesting energy with low availability at low wind speeds. There are two common types of VAWTs, that is, a Darrieus-type turbine and a Savonius-type turbine, which are driven by wind on principles of lift force and drag force, respectively. In this study, the way that the wind with higher speed impacts those VAWTs efficiently is important key to be analyzed and optimally designed while the wind at low speed is available for VAWTs.

There are very few relevant researches in attempting to improve performances of VAWTs at low speed conditions. Takao et al. (2009) developed an air flow controlling device called a "directed guide vane row". This straight-bladed

mechanism is inherently constrained due to the design; it can capture a wind stream only in a single direction of a VAWT. Pope et al. (2010) introduced numerical analysis to determine operating angles of stator vanes for a VAWT. Also, Chong et al. (2012) developed omnidirectional guide vanes, which can greatly increase power output of a VAWT. Although those devices can capture wind in all directions, optimal arrangements of guide vanes are not concerned for best practice in those studies. Additionally, it should be remarked that Ohya and Karasudani (2010) developed a shrouded horizontal axis wind turbine system called “Wind-lens turbine”. It can be learnt that wind can be speeded up by a shaped passage even though that design is not applicable to VAWTs.

### **Thailand wind Energy situation**

Modern wind turbine technology is suitable to high wind speed which is available in Europe and America. However, wind energy in Thailand is considered to be the low wind speed (Major et al., 2008). most areas of Thailand are in light blue to dark blue region which represents low wind speed compared to other color region referring to the Thailand wind resource map retrieved from Thailand Ministry of Energy as shown in Figure 1.1. Therefore, Utilization of the modern wind turbine technology is not suitable and not economic efficient because they require high capital cost and cannot generate sufficient electricity. Thus, the low speed wind turbine system which is suitable to Thailand’s wind should be developed.



		THAILAND WIND POWER CLASSES										
Elevation		1.1	1.2	1.3	1.4	2	3	4	5	6	7	
10 m	m/s	0	2.8	3.6	4.0	4.4	5.1	5.6	6.0	6.4	7.0	9.4
	W/m <sup>2</sup>	0	25	50	75	100	150	200	250	300	400	1,000
30 m	m/s	0	3.3	4.1	4.7	5.2	5.9	6.5	7.0	7.4	8.2	11.0
	W/m <sup>2</sup>	0	40	80	120	160	240	320	400	480	640	1,600
50 m	m/s	0	3.6	4.4	5.1	5.6	6.4	7.0	7.5	8.0	8.8	11.9
	W/m <sup>2</sup>	0	50	100	150	200	300	400	500	600	800	2,000

Figure 1.1 Wind resource assessment in Thailand (Ministry of Energy, 2013)

## **1.2 Purpose of study**

In this work, a wind booster is proposed for CFD-based analysis and optimization in order to improve angular speed of the VAWTs. This systematical resolution of optimal design leads to increase in mechanical power, which is generated from the VAWTs. By using optimally designed guide vanes, the wind booster can regulate flow direction and accelerate wind from any directions in order to yield the most effective impacts to VAWT blades. The optimal design of a wind booster have ability to most improve the efficiency of vertical axis wind turbine (VAWTs) in term of energy harvesting when coupling with each other. This will benefits improvement of overall usage of low available wind energy from low speed wind. To apply this study into practical usage, VAWTs with optimal wind booster can partially produce acceptable power not only from low speed wind but also enhances the potential of VAWT at higher speed wind. This helps to provide alternative energy source instead of fully using fossil fuel which will lead to less depletion of fossil fuel.

## **1.3 Significance of study**

The optimal wind booster will significantly increase mechanical power generated from a VAWT. This mechanical power can be converted to any other kinds of power used in application. This will lead to decrease in use of fossil fuel. This study intents to provide benefits to energy engineers or anyone who works or study involving wind energy. This research enlightens a way to efficiently utilize use of energy from low speed wind which is basically considered as waste energy. It provide much more benefit for countries or areas where wind speed is low, especially Thailand.

## **Chapter 2**

### **Literature Review**

As the title of this study, CFD-based analysis and optimization of wind boosters for low speed vertical axis wind turbine, there are two important keywords consisted in the title that this study focuses on. The former keyword is “vertical axis wind the turbines”. There are a few previous studies which clarify why a vertical axis wind the turbine (VAWT) should be selected over a conventional wind turbine. The latter keyword is “wind boosters” which is a kind of wind flow controlling equipment specially developed in purposed to improve mechanical power extracted from a wind turbine and is also the most essential part in this study.

#### **2.1 Vertical axis wind turbines**

Currently, most wind power systems consist of horizontal axis wind turbines (HAWTs), in mid to large-scale wind farms. These conventional turbines are often favored due to higher efficiency, but they are not necessarily suitable for all purposes.

Vertical-axis wind turbines (VAWTs) are a type of wind turbine where the main rotor shaft is set vertically and the main components are located at the base of the turbine. VAWTs are able to capture the wind from all direction and performs better in lower speed wind condition compared to HAWTs. There are two popular types of VAWT which have been used for ages. The Darrieus turbine which can generates high lift force and The Savonius turbine which can generate high drag force.

For the minimum wind speed which is used for starting the turbine, the starting torque should be concerned as essential parameters. Horizontal axis turbines (HAWTs) require sustained wind velocities to efficiently generate power. But for urban areas, especially Thailand, where wind speed is quite low and its characteristic is more turbulent due to many tall buildings in downtown. VAWTs are more reasonable choice because the ability to capture the wind from all 360 degree direction and requires less wind velocity for starting torque. Takao et al. (2009) also mentions the two additional advantages of VAWTs. The former is that the center of gravity of VAWTs is relatively

lower as the generator and gearbox can be placed on the ground and the latter is that a yaw mechanism to turn the rotor against the wind is not necessary because VAWTs can capture wind from any directions. Especially, Savonius-typed VAWTs are consider for low cost construction and produce lower noise compared to HAWT (Akwa, 2012).

## 2.2 Development of wind boosters

As the aim of the study is to improve performance of VAW, the method in this study is to shroud the VAWT with the equipment which can guide the inlet wind direction as well as increase inlet wind velocity. The equipment is called wind booster as shown in Figure 2.1.

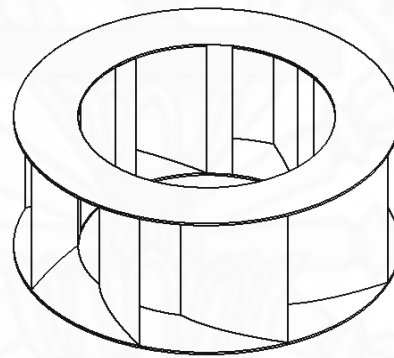


Figure 2.1 Wind booster

A wind booster is a specially designed equipment used in this study in order to improve efficiency of a VAWT. The main functions of a wind booster can be divided into two parts (Korprasertsak et al., 2014). The former is “guiding”. The guide vanes direct wind to impact VAWT blades at effective angles. The latter is “throttling”. The passages between each guide vanes is designed to throttle wind in order to accelerate the air flow before impacting VAWT blades by the principle of reduction in the area of the guide vane passages. By guiding and throttling effect of a wind booster, it is able to increase in angular velocity of VAWTs as well as mechanical power generated from VAWTs.

In literature review, there are a few studies which utilize effect of guide vanes to improve VAWT performance. Most of these designs are based on the same



principle of guiding and accelerating wind speed. Nevertheless, they are still slightly different in some details compared to this study. The past studies have investigated and confirmed that the effect of a flow controlling equipment is able to practically improve VAWT performance.

Takao et al. (2009) have developed a flow controlling equipment called as “Directed guide vane row” to equip with a straight-bladed vertical axis wind turbine (S-VAWT). Directed guide vane row consists of 3 arc plates. The experiment is tested under a wind tunnel. The guide vane is installed at the upstream wind with some gap between the guide vane and the turbine blade. Wind stream with fixed velocity is drawn to the guide vane and the S-VAWT, so that the performance of S-VAWT with the invented guide vane row can be determined by a torque detector. The effect of guide vane geometry on the performance was clarified in the study that the directed guide vane row is able to increase power coefficient and torque coefficient. However, the drawback of this design is that this design is incomplete. It can capture wind stream only in single direction and need to rotate around the VAWT blades to capture the wind from another direction that seems to be difficult for practical usage.

Pope et al. (2010) have introduced numerical methods to determine the operating performance of a VAWT. He aims to analyze effects of stator vanes on VAWTs power output. A zephyr vertical axis wind turbine (ZVWT) with 5 blades is chosen for the experiment. 9 plates of guide vane are designed covering around the turbine blades. To analyze the effect of guide vane, wind flow simulation is conducted via computational fluid dynamic (CFD) software. In addition, the researcher also invents a prototype model of the designed guide vanes and tests the wind flow through the guide vane under a wind tunnel in order to obtain practical results to support the numerical results obtained from CFD simulation. The result from the experiment is that with stator vane, the power coefficient is higher compared to without stator vane. This design now can capture the wind stream from all direction. However, it is still not clarified if this is the best design for VAWTs because of lack of proper optimization.

Chong et al. (2012) have developed Omni-directional-guide-vane (ODGV) which is mentioned that it can greatly increase the power output of the VAWT. Single-bladed Wortmann FX-63-137 VAWT is used for the experiment. The researcher optimizes the design of ODGV by using both practical experiment and numerical

experiment via CFD simulation. The dimension, numbers and guide vane plates are the variable parameters of the design optimization. Finally, the optimal design of the guide vane is presented. The optimal ODGV has 4 pairs of the guide vane plates covering around the turbine blades and the vanes in each pair are tilted at angles of  $20^\circ$  and  $55^\circ$ . The ODGV is able to capture the wind from all 360 degree direction. Not only the guide vanes are able control the direction of upstream wind, but also reducing in area of each guide vane channel that can increase wind velocity before impact the turbine blade. The experimental results show that the rotational speed of the VAWT increases by about 2 times. Simulations show that the installation of the ODGV increases the torque output of a single-bladed VAWT by 206%. However, the shape of this design is not symmetric for all direction, the increment of power still depends on the direction of upstream wind.

Yuji Ohya et al. (2010) has been developed the shrouded HAWT system called “Wind-lens turbine”. Wind-lens turbine consists of a diffuser shroud with a broad-ring brim at the exit periphery and a HAWT inside it. The shrouded HAWT with a brimmed diffuser has demonstrated power augmentation for a given turbine diameter and wind speed by a factor of about two to five compared with a bare HAWT. This is because a low-pressure region due to a strong vortex formation behind the broad brim draws more mass flow to the wind turbine inside the diffuser shroud.

In summary, there are a few past studies which prove that the effect of various equipment is able to improve VAWTs performance. It is generally designed based on 2 main principles which are guiding and accelerating of the upstream wind to increase angular speed of VAWT leading to increment in generated mechanical power. However, There are still some drawbacks in each previous design, so there are still exist gaps that need to be improved and well optimized in order to achieve the best design for practical usage.

This study performs the design and the method of optimization of wind boosters for low speed vertical axis wind turbine to achieve increment in performance as well as mechanical power generated from VAWTs as high as possible. It aims to overcome or at least reduce the drawbacks of the previous studies, so that the turbines are able to operate in low speed wind condition more practically and more efficiently.

## **Chapter 3**

### **Methodology**

In this study, the analysis and optimization of a designed wind booster in order to find out which design of the wind booster will most increase mechanical power VAWT in low speed wind condition. The experiment including modeling and design of the wind booster is mainly based on computational fluid dynamics (CFD) by utilizing XFlow™ CFD (Next Limit Technologies, 2015) software which is a reliable CFD software and suitable to simulate and compute the external flow problem. Also, the CFD-based experiment has so many advantages which can bypass some limitation in performing the experiment. For example, The CFD-based method help to reduce large amount of budget and time in modelling a VAWT, a wind booster and especially a wind tunnel which has very high cost and is not much available at any institute.

The scope of this study is in the range from modeling a preliminary wind booster design which will couple to a simple Savonius VAWT as a case study model to analysis of improvement in performance of a VAWT by effect of a designed wind booster and finally, the optimization of a related parameter of a wind booster is performed to achieve an optimal design which is able to most improve a VAWT performance. Some additional experiment is also performed to support the reliability of the CFD results in the study.

#### **3.1 Modelling and design of wind boosters**

In this study, CFD-based simulation of a VAWT coupled with a specially-designed wind booster is performed in order to analyze what effects on air streams that lead to an increase in the overall angular speed of a VAWT at low wind speed conditions of 1 m/s to 8 m/s. Actually, there is another typical method, which is able to increase mechanical power output of VAWT by enlarging size of turbine. However, the reasons to increase wind speed are:

1) The relationship between wind speed and wind power is “power is proportional to wind speed power three”; therefore, increasing wind speed can greatly multiply power output of a VAWT compared with an increase in size of a turbine. The available wind power equation can be derived as shown below.

Wind is made up of moving air molecules which have mass. Any moving object with mass carries kinetic energy in an amount which is expressed by the equation:

$$E_k = \frac{1}{2}mv^2 \quad (3.1)$$

where  $E_k$  is the kinetic energy (J),  $m$  is the mass of air (kg), and  $v$  is the velocity of air (m/s).

The wind mass flowing to a VAWT per second is given by the following equation:

$$\dot{m} = \rho v A \quad (3.2)$$

where  $\dot{m}$  is the mass flow rate of air (kg/s),  $\rho$  is the air density (kg/m<sup>3</sup>), and  $A$  is the frontal area of VAWT (m<sup>2</sup>).

By substituting mass flow rate calculation into the standard kinetic energy equation (3.1) given above. The available power in wind hitting a VAWT with a certain frontal area is:

$$P = \frac{1}{2}\rho A v^3 \quad (3.3)$$

where  $P$  is the available wind power (W).

2) This method does not require a large wind turbine, which means savings both cost for material and space for installation. Also, it may not be workable at low wind speed owing to hard start-up of large inertia.

By utilizing SolidWorks CAD software, the preliminary design of a wind boosters as well as a simple VAWT is modelled as a case study. Note that the models are saved as .STEP format in order to make them be able to import to CFD software for wind analysis later on.

The concept for designing a wind booster is to not only guide wind to blades of a VAWT but also increase wind speed before engaging to a VAWT. As shown in Figure 3.1, guide vanes with curve sided triangle shape are designed to direct air streams to turbine blades properly. To increase wind speed, the guide vanes are arranged to throttle air streams. Since wind can blow to all 360 degree direction of a VAWT, the blades of guide vanes are set up around a VAWT. The upper and lower rings are used to fix all the guide vanes at certain positions around the wind turbine.

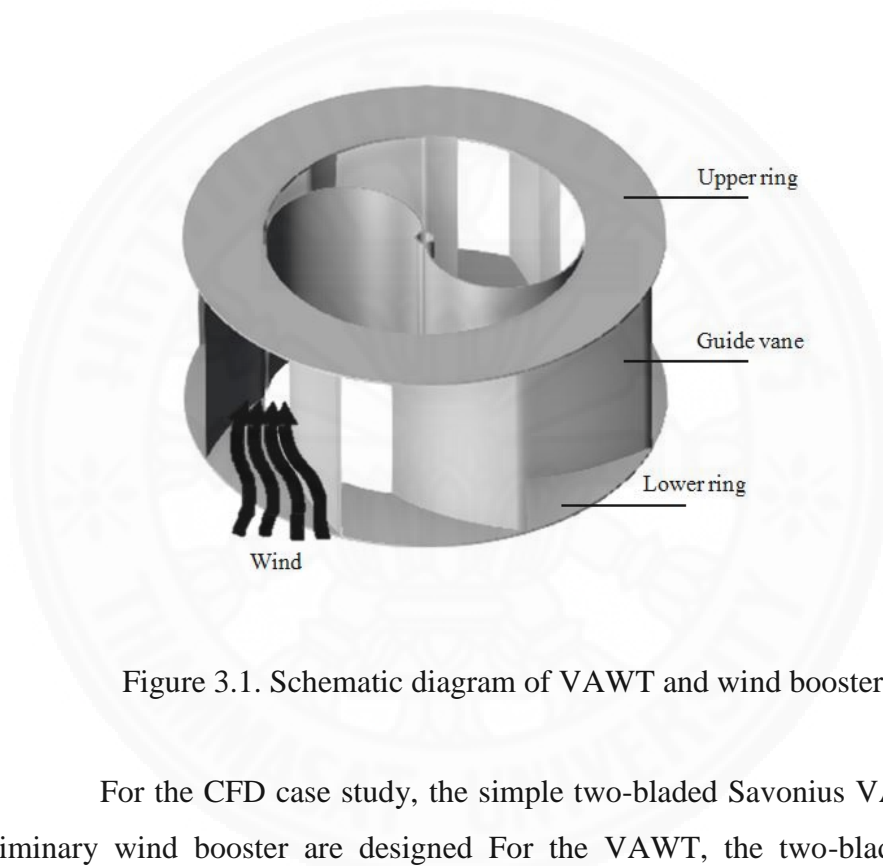


Figure 3.1. Schematic diagram of VAWT and wind booster

For the CFD case study, the simple two-bladed Savonius VAWT and the preliminary wind booster are designed. For the VAWT, the two-bladed Savonius VAWT is chosen for the case study as it can be simply modeled and has higher performance compared to the three-bladed type (Ali, 2013). Although it has been studied that Savonius VAWTs lack the ability to generate high mechanical power compared to Darrius VAWTs, on the other hand, Savonius VAWTs are much less complicated to be modeled and also, the mechanism to generate mechanical power from wind energy is less complicated thanks to the drag-type blades of Savonius VAWT. However, this study is not only specific to Savonius VAWT. Any kinds of VAWT could be benefited by this study as the wind booster is designed to improve the mechanical power from any VAWTs. The preliminary wind booster is designed which

the eight guide vanes of the wind booster are curved side triangle shape with the leading angle of  $60^\circ$  as shown in Figure 3.2. Note that this preliminary design of wind booster is still not well optimized. It will be taken into the optimization process later.

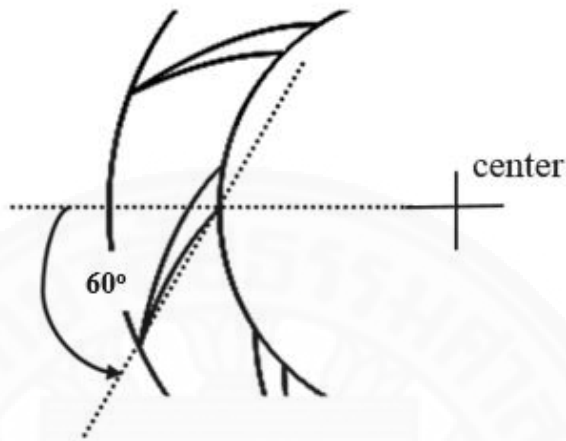


Figure 3.2 Leading angle of the preliminary wind booster

Table 3.1 and Figure 3.3 show the specification of the Savonius VAWT and Table 3.2 and Figure 3.4 show the specification of the preliminary wind booster. The size is in mm.

Table 3.1 Specification of the VAWT

Parameters	Values
Core diameter	25 mm
Core thickness	3 mm
Blade radius	97 mm
Blade thickness	2 mm
Blade height	250 mm

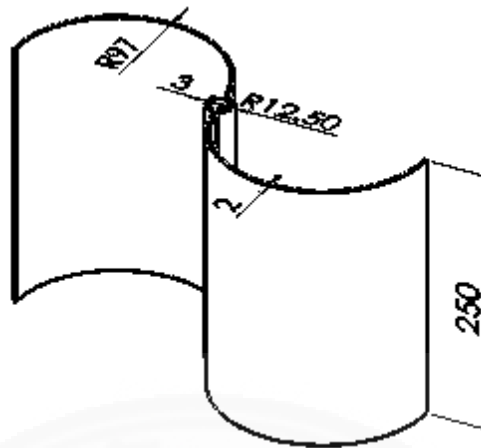


Figure 3.3 Dimension of the VAWT

Table 3.2 Specification of the wind booster

Parameters	Values
Booster outer diameter	600 mm
Booster inner diameter	400 mm
Number of guide vane	8 blades
Booster height	250 mm

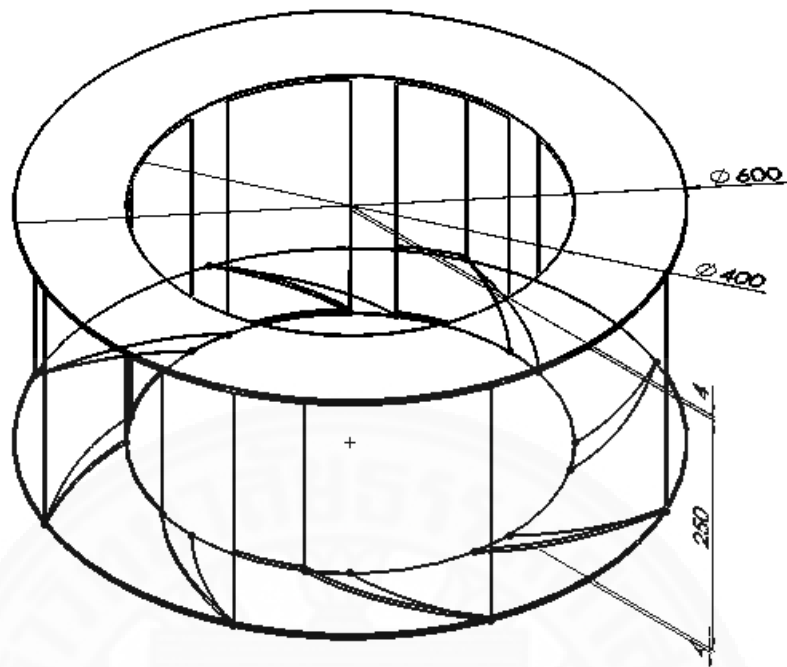


Figure 3.4 Dimension of the wind booster

Figure 3.5 shows the assembly of the VAWT and the wind booster. The wind booster is mounted at the middle of the VAWT which allows the VAWT rotates in vertical axis when subjected to wind force.

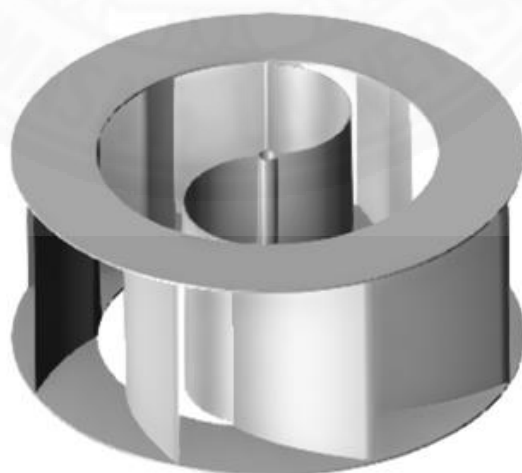


Figure 3.5 Assembly of the VAWT and the wind booster



### 3.2 Power analysis on VAWTs

The power analysis of a VAWT is presented for understanding efficiency of the VAWT with/without wind booster, which is defined with the coefficient of power. Conceptually, this inherent characteristic of a given VAWT is adapted after installing a wind booster.

In wind power analysis on VAWT, wind energy can convert into the mechanical power via the mechanism of a VAWT subjected to a generator. Basically, the generator operates with higher torque when the VAWT is exert by higher wind force or higher wind speed. The mechanical power output from the VAWT can be determined by multiplication of torque and the operating rotational speed of the generator. The generator operating speed is equal to the VAWT angular speed as the VAWT and the generator are generally linked to each other with the same shaft. Hence the VAWT power output can be express by:

$$P_T = T\omega \quad (3.4)$$

where  $P_T$  is the power output of the VAWT,  $T$  is the torque of the VAWT (Nm) and  $\omega$  is the angular speed of the VAWT shaft (rad/s).

Wind energy is the kinetic energy of air, which is partially recovered by the VAWT. In other words, the power output of the VAWT cannot be entirely recuperated for mechanical power. The coefficient of power is known as the fraction of the power output extracted from the power in the wind by the VAWT. In the theory of Betz, the coefficient of power is always not greater than  $16/27(0.59)$ . This inherent characteristic of a given VAWT can be used as efficiency of the VAWT. The coefficient of power is defined as:

$$C_p = \frac{P_T}{P} \quad (3.5)$$

where is  $C_p$  the coefficient of power.

In wind power analysis, the coefficient of power is usually presented as a function of the tip speed ratio. The tip speed ratio is the ratio of the speed of the ending tip of the VAWT blade to the wind speed. It can be written as:

$$\lambda = \frac{r\omega}{v} \quad (3.6)$$

where  $\lambda$  is the tip speed ratio,  $r$  is the radius of the VAWT blade (m).

### 3.3 CFD-based analysis on VAWTs and wind boosters

For CFD case studies, a savonius-type VAWT and a wind booster (see Figure 3.3 and Figure 3.4) are investigated for genuine performances of mechanical behaviors. The material in modeling the VAWT is proposed to be a fiber plastic of 1000 kg/m<sup>3</sup>. The assembly under working conditions is illustrated in Figure 3.5. The VAWT is mounted at the middle of the wind booster. It rotates about the vertical axis while the wind booster is fixed at the position.

The experiments are performed with CFD-based simulations by utilizing XFlow<sup>TM</sup> CFD software [5] which is a reliable CFD software and suitable to simulate and compute the external flow problem. To investigate how the wind booster has effect on the change of wind stream described by change in wind velocity and wind direction, the standalone wind booster is firstly tested under the wind stream of 3 m/s which represents the average low wind speed of Thailand. Next, the stand-alone VAWT and the VAWT equipped with the wind booster are tested to investigate different performances on mechanical works. The simulations are divided into two cases: 1.) no loading condition and 2.) various loading conditions. In simulations, the wind speed is varied from 1 m/s to 8 m/s for low wind speed conditions. The VAWT is to turn in clockwise direction of the vertical axis under the frictionless rotation. For various loading conditions, external torques are applied to a shaft of the VAWT in counter clockwise direction as shown in Figure 3.6.

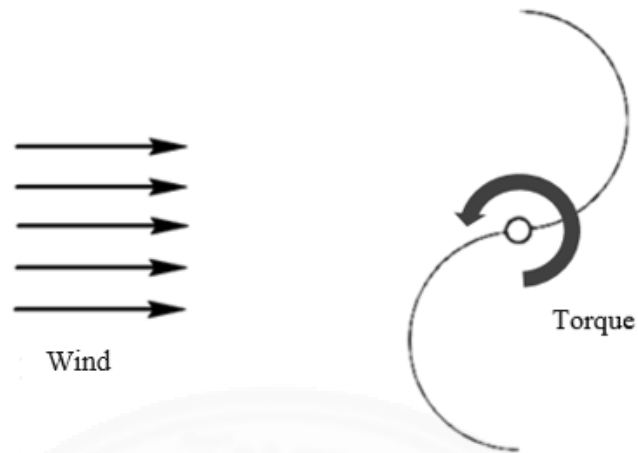


Figure 3.6 VAWT exerted by external torques

### 3.3.1 CFD Simulation setup

This section explained how the model is set to simulate VAWT which rotates by the effect of wind force by utilizing XFlow<sup>TM</sup> CFD software as shown Figure 3.7. The first step is to import the model of the VAWT and the wind booster from the CAD software to the CFD software as the geometry of the CFD simulation. The format of model files is saved to .STEP as XFlow<sup>TM</sup> CFD supports this format type. Thanks to the particle-based approach behind XFlow<sup>TM</sup> CFD, Meshing process can be skipped unlike another conventional CFD software with mesh-based approach (Musavi and Ashrafizaadeh, 2015). Usually, it is quite complicate to simulate moving part in conventional CFD software, However it is very straight forward to perform in the particle-based CFD software. The setup of simulation parameter in XFlow<sup>TM</sup> CFD are divided into four major steps which are environment setup, material setup, geometry setup and simulation setup respectively.

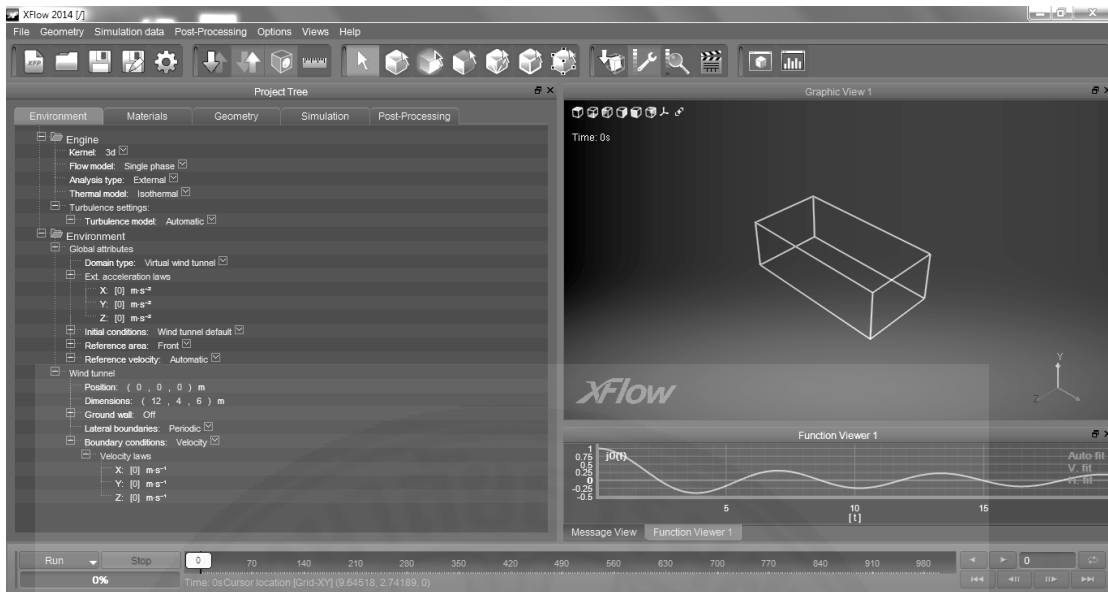


Figure 3.7. XFlow™ CFD's user interface

In environment setup, three-dimension analysis is preferred in this CFD study as it is much more practical for wind analysis compared to two-dimension analysis. This case of wind analysis is classified as the external flow model and the fluid (air) temperature is assumed to be constant. Therefore the flow model, the analysis type, and the thermal model is set to be single phase, external, and isothermal respectively. For turbulence model, it is automatically set to be Wall-Adapting Local Eddy model (WALE) with the WALE constant ( $C_w$ ) of 0.325 typically. WALE is one of Large Eddy simulation (LES) approach known as an appropriate method for simulating three dimension aerodynamic providing decent accuracy with acceptable computing time (Wang et al., 2010). The virtual wind tunnel can be directly set to mimic the real wind tunnel with VAWT and wind booster inside. Also, Wind speed and direction can be set in the virtual wind tunnel. The virtual wind tunnel is set to be large enough for allowing the turbine is able to generate wake of wind stream. It should be noted that too large size of wind tunnel cause increasing in unnecessary computing time.

In material setup, the property of the fluid type is set to be air with molecular weight, density, and operating temperature of 28.97 g/mol, 1.225 kg/m<sup>3</sup>, and

288.15 K respectively. The viscosity model is Newtonian with dynamic viscosity of 0.00018 Pa·s based on the air property.

In geometry setup, the VAWT and wind booster model were imported to the software. The VAWT is set to locate at the center of the wind booster. The geometry behavior of the VAWT is set to be rigid body dynamic in order to allow the VAWT can be set to be able to rotate in vertical direction while the geometry behavior of the wind booster is set to be fixed for non-moving part. The VAWT material density is set to be a fiber plastic of 1000 kg/m<sup>3</sup> for the study case.

In simulation setup, the simulation time is set to be sufficient to simulate the VAWT from transient state until steady state. Courant number is the feature in XFlow<sup>TM</sup> CFD indicating the size of time step in simulation process. Smaller time step results in higher accuracy of the simulation but causes increasing in the computing time. The suitable courant number for this case study is 1 to 2 which provides acceptable accuracy and computing time. The resolved scale indicates the resolution of the fluid on the simulation. Like the time step, smaller number of resolved scale provides higher accuracy of the results but cause increasing in the computing time. For this CFD case study, the suitable far-field resolved scale and near-wall resolve scale are 0.08 m and 0.02 m respectively.

Table 3.3 shows the summary of all major parameters setup which is typically used in every CFD-based simulations for this study.

Table 3.3 Simulation setup

Parameters	Values
Kernel	3D
Flow model	Single phase external
Thermal model	Isothermal
Turbulence model	Wall-Adapting Local-Eddy (WALE)
Domain type	Virtual wind tunnel
Fluid Type	Air
Fluid molecular weight	28.97 g/mol
Fluid density	1.225 kg/m <sup>3</sup>
Fluid Temperature	288.15 K
Viscosity model	Newtonian
Fluid dynamic viscosity	0.00018 Pa·s

Geometry behavior (VAWT)	Rigid body dynamic
VAWT rotation axis	Vertical
VAWT density	1000 kg/m <sup>3</sup>
Geometry behavior (wind booster)	Fixed
Courant number	1-2
Far field resolved scale	0.08 m
Near wall resolved scale	0.02 m

### 3.4 Optimization algorithm

After performing the analysis of the VAWT and the preliminary wind booster via CFD-based simulation in section 3.3. The wind booster is taken into optimization process in order to find the optimal design which is able to improve the VAWT performance for low speed wind as much as possible.

Figure 3.8 shows a graphical example of plots of the coefficient of power against the tip speed ratio. It can be observed that the curve of the coefficient of power in a case of incorporating with wind booster is higher than the curve in a case of no wind booster since the wind is expected to blow at higher speed. Additionally, the efficiency of the VAWT can be improved by maximizing the value of the coefficient of power. This enhancement can be done with the selection of best components of the wind booster from available alternatives such as number, shape, leading angle of the guide vane.

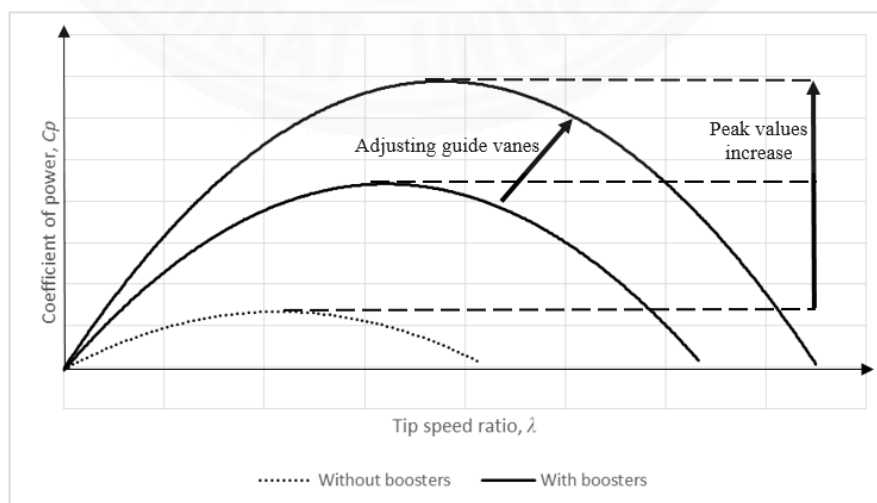


Figure 3.8 Typical plots of coefficient of power against tip speed ratio

In accordance of figure 3.8, it can be observed that number, shape, and leading angle of the guide vane are regarded as design variables in optimization. It can be obviously seen that the shape of the guide vane is the qualitative variable, which cannot be numerically determined for optimal results. Hence, the potential shapes are proposed in structures of curved side triangle, straight side triangle, straight line as shown in Figure 3.9, 3.10, and 3.11, respectively, as the optimization cases.

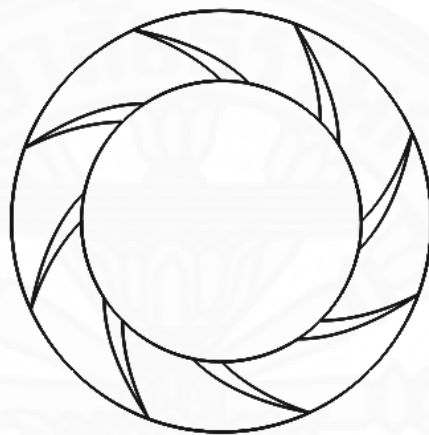


Figure 3.9 The wind booster with curved side triangle shape of guide vane

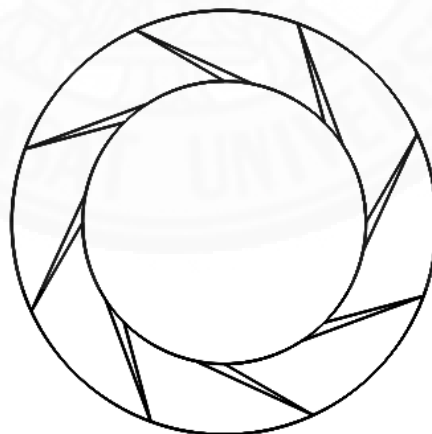


Figure 3.10 The wind booster with straight side triangle shape of guide vane

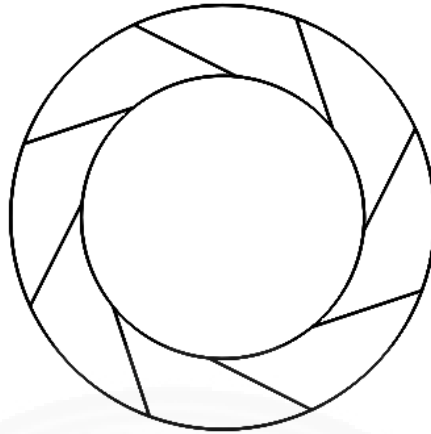


Figure 3.11 The wind booster with straight line shape of guide vane

On the other hand, leading angle of the guide vane  $\alpha$  and number of the guide vane  $\beta$  can be considered quantitative variables. The number of the guide vane is set to be integer greater than 0 while the leading angle of guide vane is defined in real values between  $0^\circ$  and  $90^\circ$  as shown in Figure 3.12.

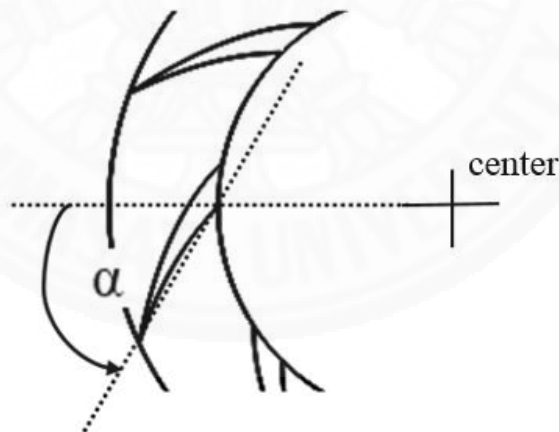


Figure 3.12 Leading angle of guide vane

In the optimization of the wind booster, the aim is to maximize the peak value of coefficient of power  $\hat{C}_p$ . The objective function  $f$  with the design variables and the constraint for the optimization are defined as:



$$\text{Maximize } \hat{C}_p = f(x)$$

$$\text{Constraints: } x \in [\alpha \ \beta]^T, \alpha \in [0,90], \beta > 0$$

It should be noted that the peak value of coefficient of power  $\hat{C}_p$  can be roughly predicted from no-load speed and maximum torque of VAWT (see Appendix A).

The alternating direction technique is effectively implemented to exploratory and pattern searches for optimal solutions by performing CFD experiments (Leephakpreeda, 2000). It does not require gradient of the objective function rather than the value of the objective function in searching. For given values of design variables, the peak value of the coefficient of power is determined for each evaluation of the objective function. The principle is based on that any point on n-dimensional search space can be reached from any starting point by linking along the axis by n times. This technique relies on utilizing two types of moving which are exploratory move and pattern move to eventually reach the optimum point. The exploratory move is the movement that either optimization variable  $\alpha$  or  $\beta$  is varied while the pattern move both optimization variables  $\alpha$  and  $\beta$  are varied as illustrated in Figure 3.13.

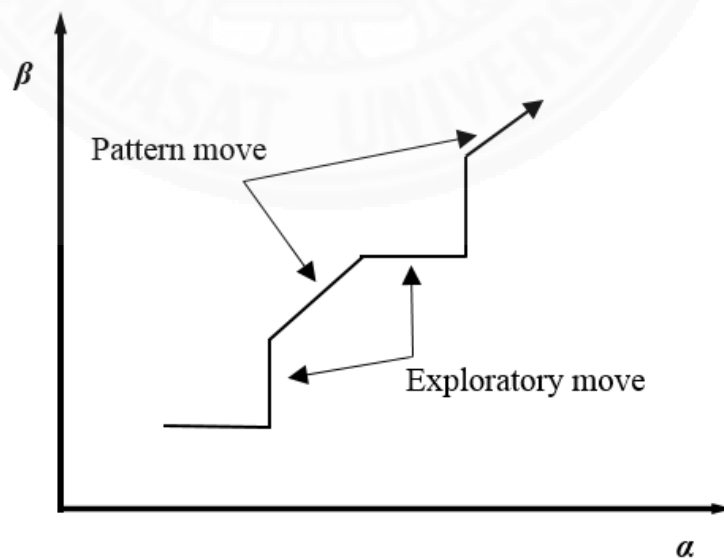


Figure 3.13 Alternating direction technique in CFD experiments

The algorithm of the alternating direction technique for finding a maximum point is explained in steps as follows:

Step 1. Define  $x^{(k=0)}$  as the estimated maximum point at  $i = 1$ ,  $\delta$  is the magnitude of step for each design variable,  $\varepsilon$  is the accuracy of maximum objective function value,  $i$  is the order index of design variables, and  $k$  is the iteration index.

Step 2. Find maximum value of  $f(x^{(k)})$ ,  $f(x^{(k)} - \delta e)$ , and  $f(x^{(k)} + \delta e)$  where  $e = [0_1 \ 0_2 \ \dots \ 1_i \ \dots \ 0_n]^T$  and  $n$  is the total dimension of design variables.

Step 3. Define  $k = k + 1$  and  $x^{(k)}$  is maximum point in step 2

Step 4. If  $i \neq n$ , define  $i = i + 1$  and move to step 2 or else define  $i = 1$  and move to step 5 (exploratory move).

Step 5. If  $x^{(k)} \neq x^{(k-1)}$  move to step 7 or else move to step 6.

Step 6. If  $\delta < \varepsilon$ , stop Iteration or else reduce  $\delta$  and move to step 2.

Step 7. Define  $k = k + 1$  and  $x^{(k)} = 2x^{(k-1)} - x^{(k-3)}$  (pattern move).

Step 8. If  $f(x^{(k)}) > f(x^{(k-1)})$ , move to step 7 or else define  $x^{(k)} = x^{(k-1)}$  and move to step 2

The mentioned algorithm in seven step above can be clearly demonstrated by a flow chart diagram as shown in Figure 3.14.

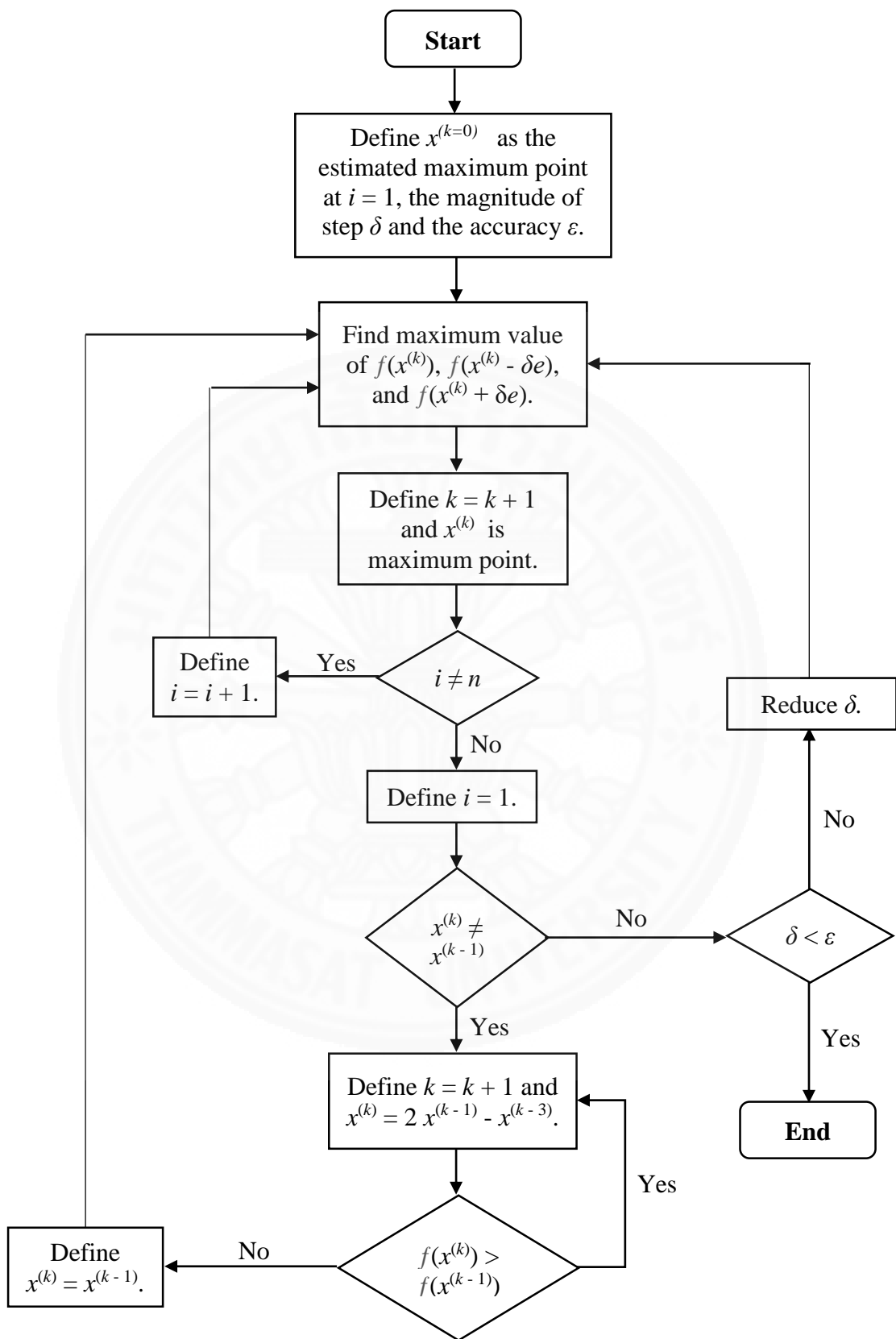


Figure 3.14 Algorithm of alternating direction technique

## Chapter 4

### Results and Discussion

#### 4.1 Performance analysis on VAWTs and VAWT with wind boosters

The experiments of VAWT rotations are performed with CFD-based simulations by utilizing XFlow™ CFD software. For CFD experiments, a Savonius-type VAWT and a preliminary design of wind booster are investigated for genuine performances of mechanical behaviors. The dimensions of the VAWT and the designed wind booster are shown in Fig. 3.5. The material in modeling the VAWT is proposed to be a fiber plastic of  $1000 \text{ kg/m}^3$ . The VAWT is mounted at the middle of the wind booster. Rotations of the VAWT are taken into account under external flow condition. It rotates about the vertical axis while the wind booster is fixed at the position.

To investigate how the wind booster influences on the change of wind stream, which is described by change in wind speed and wind direction, the standalone VAWT and the VAWT equipped with the wind booster are tested on mechanical works. In simulations, the wind speed is varied from 1 m/s to 8 m/s for low wind speed conditions. The VAWT is to turn in clockwise direction of the vertical axis under the frictionless rotation. Fig. 4.2 and Fig. 4.3 show examples of CFD simulations for a given time on steady state rotations of the standalone VAWT and the VAWT with the wind booster, respectively. The conducted wind of 3 m/s is set to flow from the left side to the right side. The gray vector represents the velocity of wind where the arrow head indicates the direction of wind and the gray color represents the magnitude of the wind. It can be observed that the VAWT is turned in clockwise direction at a given speed.

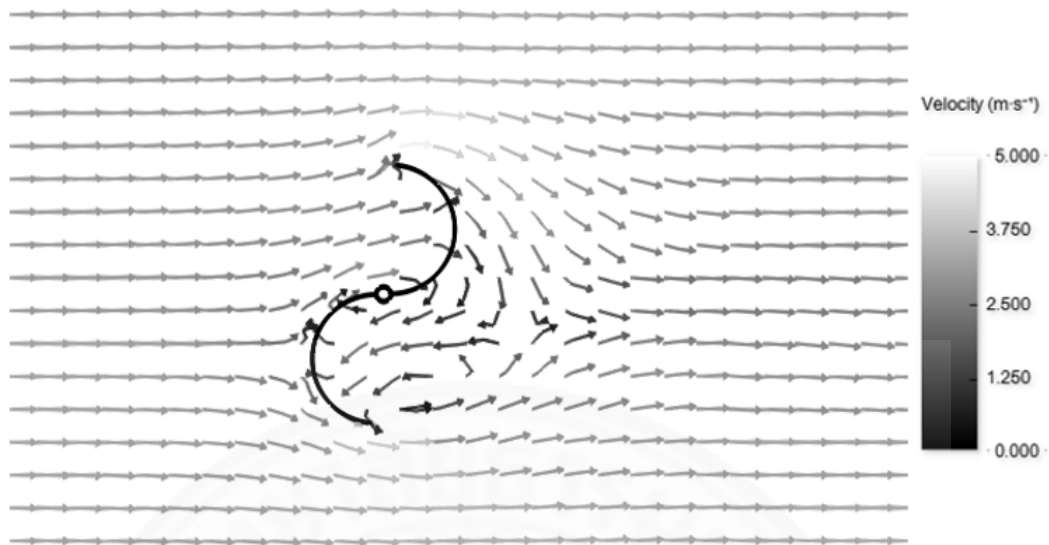


Figure 4.1 CFD simulation of VAWT without wind booster

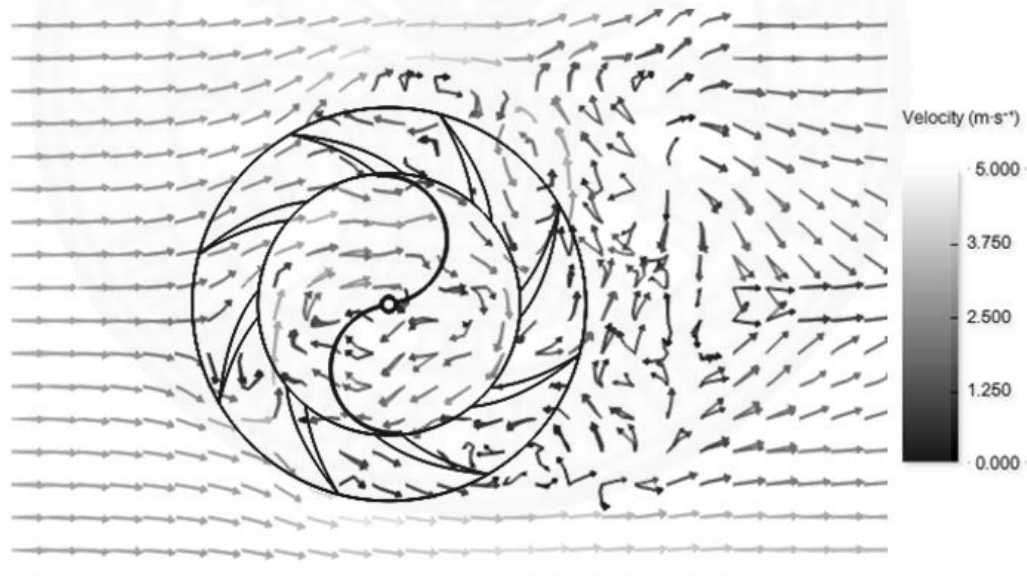


Figure 4.2 CFD simulation of VAWT with wind booster

#### 4.1.1 Mechanism of wind booster

The main mechanism of a wind booster, as shown in Figure 5, can be separated into two functions. The former is “guiding”; the guide vanes direct wind to impact VAWT blades at effective angles. The latter is “throttling”; the passage between

each guide vane is set up to throttle air flow to be accelerated before impacting VAWT blades.

The simulated results in Figure 4.3 show that when the air at the region A flows along a positive X axis through the wind booster, the guide vanes lead the wind to the VAWT blades at the region B. The VAWT blades are effectively pushed by the wind in this region. Also, the guide vanes prevent the wind countering rotation of VAWT at the region C. The passage between two guide vanes is designed to throttle the wind in order to increase the wind speed. The wind speed at the region B is higher than the region A.

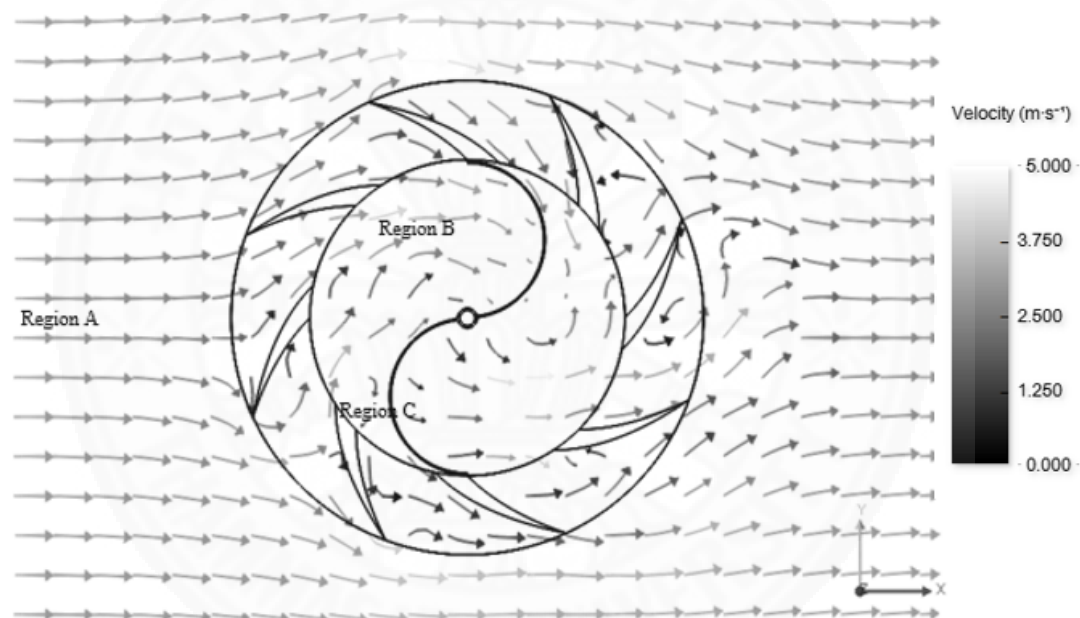


Figure 4.3 Wind flowing through VAWT with the wind booster

#### 4.1.2 VAWTs and wind boosters in no loading condition

Under no loading condition, the simulated results on angular speed of the VAWT are reported in Table 4.1. Note that the VAWT angular speeds are measured at the steady state of rotation (see Appendix B). The wind booster is capable of increasing angular speeds of the VAWT by approximately greater than 50% of angular speeds of the VAWT without the wind booster at various wind speeds. It can be observed that

the increment in the VAWT's angular speed is boosted up from effects of throttling and guiding from the proposed booster.

Table 4.1 Angular Speeds of VAWT at various wind speeds

Wind Speed (m/s)	Angular speed (RPM)		Increment (%)
	Without booster	With booster	
1	19.6	29.7	50.97
2	39.2	59.6	52.07
3	59.5	90.7	52.24
4	78.5	120.1	52.86
5	98.4	151.2	53.64
6	118.0	180.4	52.91
7	138.6	210.9	52.13
8	158.6	240.2	51.48

The plots of the angular speeds of the VAWT are graphically shown in Figure 4.4. The curve of the VAWT speed in the case of the VAWT with the wind booster significantly shifts over the curve of the VAWT speed in the case of the VAWT without the wind booster. This increment in angular speed of the VAWT results in great improvement of mechanical power generation.

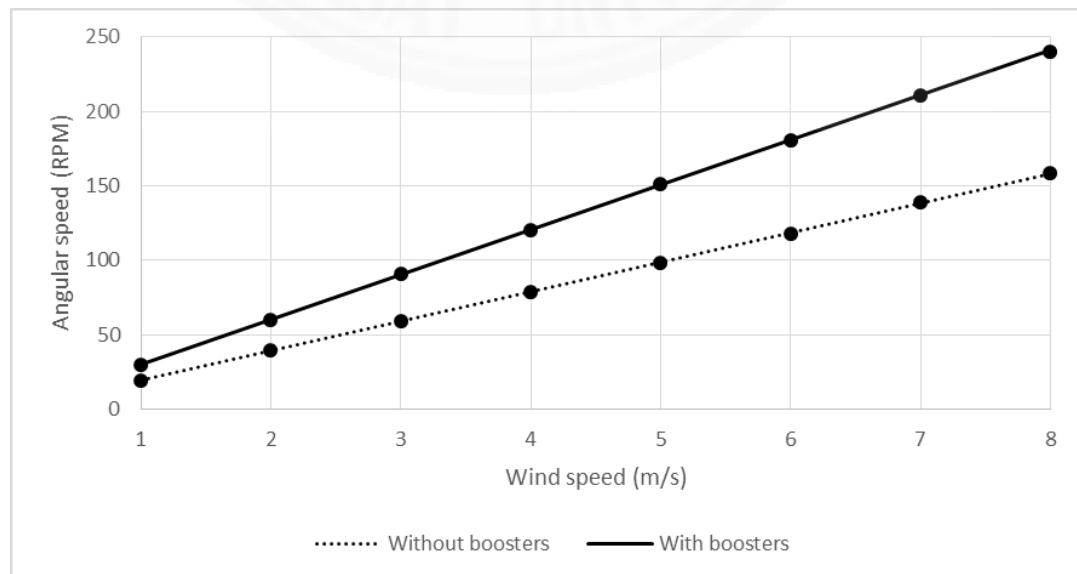


Figure 4.4 Plots of VAWT angular speed against wind speed

For providing preliminary validation, the wind turbine and the wind booster are simply constructed from the acrylic plastic. The standalone VAWT and the VAWT with wind booster are tested under the wind stream of 2-7 m/s blowing directly from variable speed fan to VAWTs as shown in Figure 4.5. The wind speed is measured by an hand held anemometer and the VAWTs' angular speed is measured by a tachometer. The measurements of the mean wind speed are located at the mid-front of the wind turbine.



Figure 4.5 VAWT with wind booster during the experiment process

The results are as shown in Figure 4.6. The increment of the VAWT's angular speed is about 20% which is less than the increment found in CFD study because the fan used as wind source is not able to generate uniform wind steam like in the CFD simulation and this fan is not able to generate enough large stream due to its



small size. However, the results are still agreed with the CFD one as both have similar characteristic of the increment.

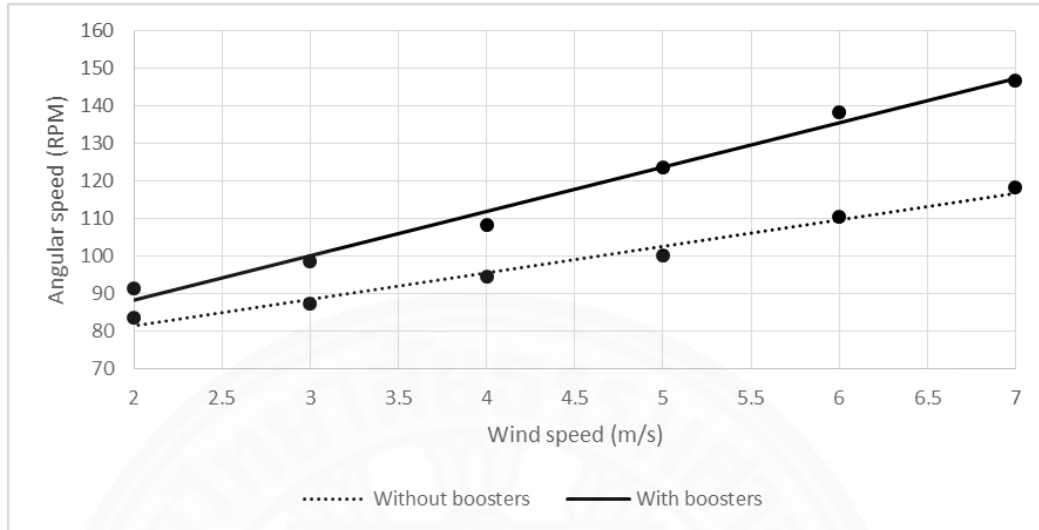


Figure 4.6 Plots of VAWT angular speed against wind speed (Experimental case)

To investigate practical usage of the wind booster, the additional CFD experiments are performed by simulating the VAWT under real wind conditions. The measurements of wind speed are recorded at the SIIT main building at the height of 3 m from the ground by a three-cup anemometer as shown in Figure 4.7.



Figure 4.7 Working three-cup anemometer in wind measurement

The wind conditions present a circumstance that the wind blows in urban area at low speed. The data of wind speed is collected every 10 second. The 20-minutes wind data (see Figure 4.8) is inputted to CFD model in simulation. The wind speed fluctuates over the time. It can be noticed that the mean wind speed of 0.5 m/s is very low. The simulated results in Figure 4.9 shows that the VAWT coupled with wind booster performs greater mechanical works in terms of the VAWT angular speeds than the standalone VAWT. However, at extremely weak wind ( $< 0.2$  m/s), the standalone VAWT performs better. This can be explained by the wind booster becoming an obstacle under very low wind speed conditions. In this situation, the availability of the wind is actually negligible to do practical works.

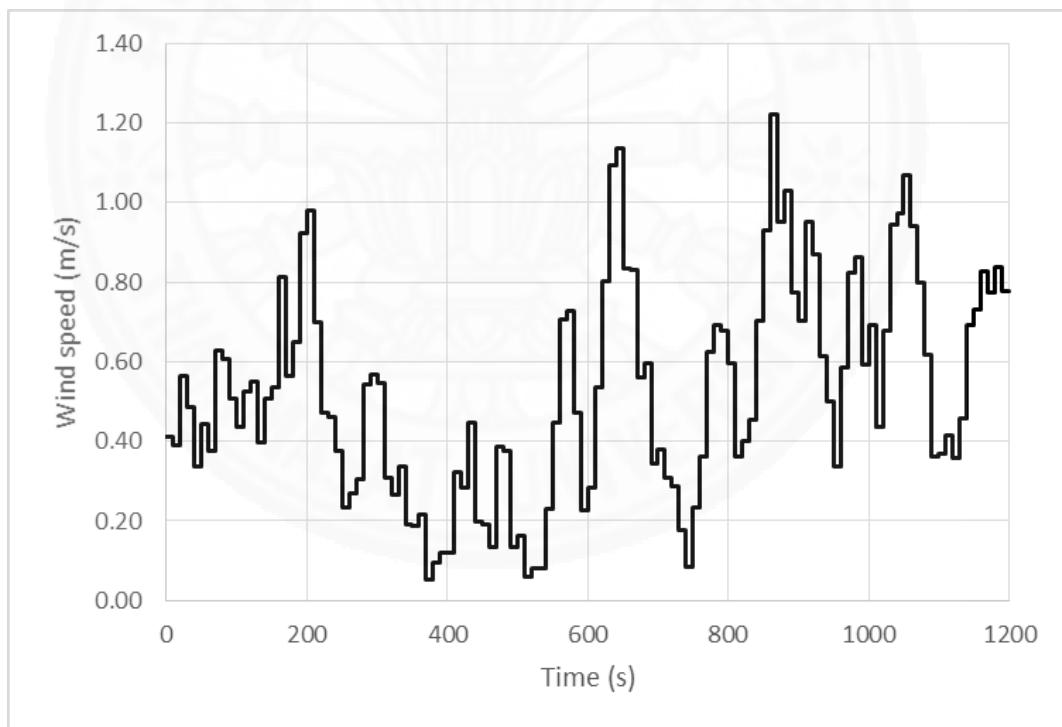


Figure 4.8 Input wind speed in CFD simulation

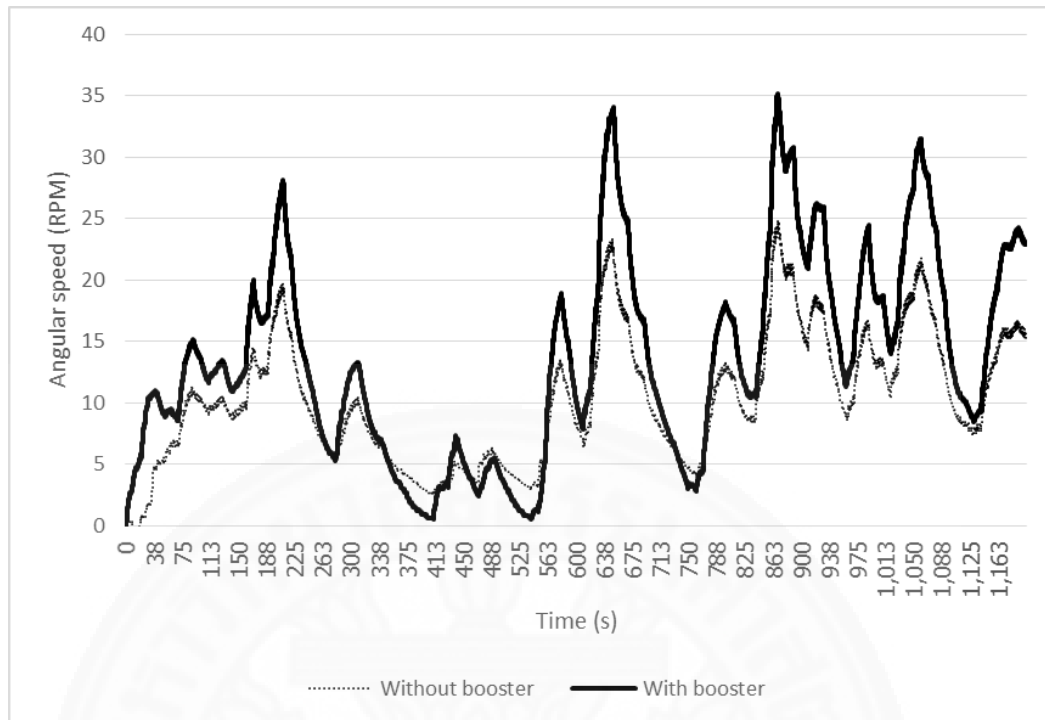


Figure 4.9 Plot of VAWT speed against time for 0.5 m/s of average wind input

The higher wind speed is of interest in this study. Therefore, the measurement of the wind in Fig. 4.8 is shifted up in magnitude so that the mean wind speed is about 3 m/s before it is inputted to the CFD model again. The simulated results, as depicted in Fig 4.10, show that the VAWT coupled with the wind booster is capable of rotating with higher angular speed than the standalone VAWT all times. It can be noticed that the entire curve of the angular speed of the VAWT coupled with wind booster shifts over the curve of the angular speed of the standalone VAWT.

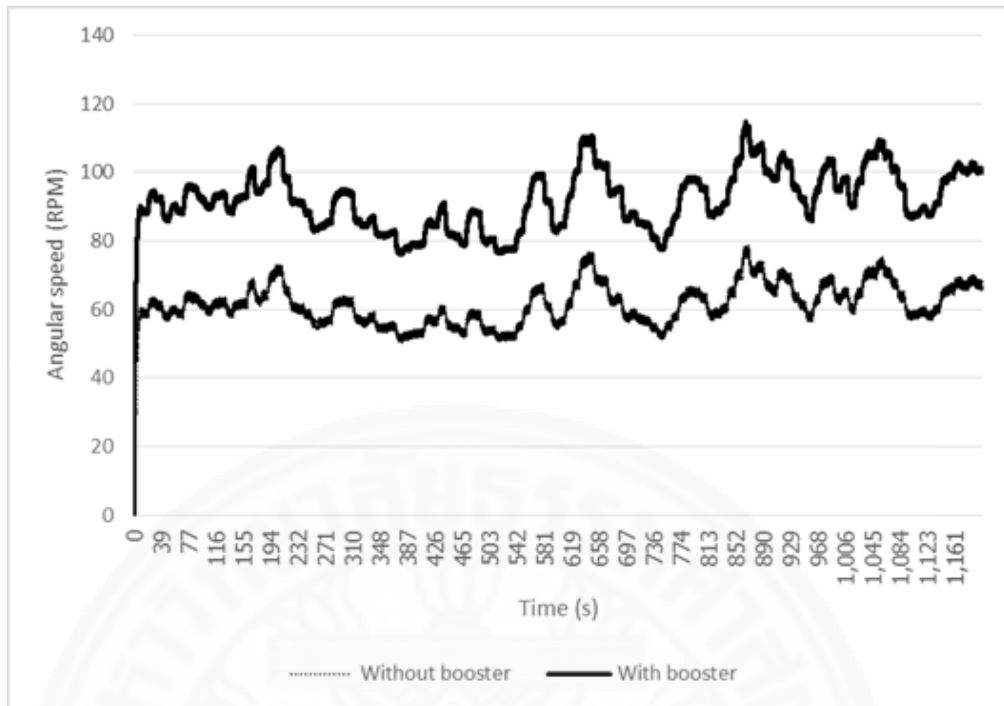


Figure 4.10 Plot of VAWT speed against time for 3 m/s of average wind input

#### 4.1.3 VAWTs and wind boosters in various loading condition

For various loading conditions, external torques are applied to a shaft of the VAWT in counter clockwise direction in CFD experiments as shown in Figure 3.6. The results of torque against and mechanical power against VAWT angular speed are reported on Table 4.2.

Table 4.2 Torque and mechanical power against VAWT speed at various wind speed

Wind speed (m/s)	Without boosters			With boosters		
	Speed (rad/s)	Torque (Nm)	Power (W)	Speed (rad/s)	Torque (Nm)	Power (W)
	0	0.0012	0	0	0.003	0
1	0.55	0.001	0.00055	0.63	0.0026	0.001638
	0.88	0.0008	0.000704	0.96	0.0022	0.002112
	1.31	0.0006	0.000786	1.31	0.0018	0.002358
	1.62	0.0004	0.000648	1.75	0.0014	0.00245

	1.84	0.0002	0.000368	2.18	0.001	0.00218
	2.06	0	0	2.68	0.0006	0.001608
				2.97	0.0002	0.000594
				3.11	0	0
	0	0.005	0	0	0.013	0
	1.37	0.004	0.00548	0.91	0.011	0.01001
	1.88	0.003	0.00564	2.01	0.009	0.01809
2	2.95	0.002	0.0059	3.03	0.007	0.02121
	3.54	0.001	0.00354	3.86	0.005	0.0193
	4.11	0	0	5.16	0.003	0.01548
				5.89	0.001	0.00589
				6.25	0	0
	0	0.0125	0	0	0.0275	0
	1.6	0.01	0.016	2.32	0.0225	0.0522
	2.56	0.0075	0.0192	4.05	0.0175	0.070875
3	4.27	0.005	0.02135	5.43	0.0125	0.067875
	5.4	0.0025	0.0135	7.56	0.0075	0.0567
	6.24	0	0	8.77	0.0025	0.021925
				9.5	0	0
	0	0.02	0	0	0.05	0
	2.04	0.0175	0.0357	1.5	0.045	0.0675
	2.58	0.015	0.0387	3.18	0.04	0.1272
	3.67	0.0125	0.045875	5.61	0.03	0.1683
4	5.24	0.01	0.0524	7.71	0.02	0.1542
	6.13	0.0075	0.045975	10.82	0.01	0.1082
	6.95	0.005	0.03475	12.58	0	0
	7.74	0.0025	0.01935			
	8.23	0	0			
	0	0.03	0	0	0.08	0
	2.36	0.0275	0.0649	2.21	0.07	0.1547
5	3.58	0.0225	0.08055	4.44	0.06	0.2664
	5.72	0.0175	0.1001	6.38	0.05	0.319
	7.42	0.0125	0.09275	8.1	0.04	0.324

	8.85	0.0075	0.066375	9.93	0.03	0.2979
	9.88	0.0025	0.0247	12.77	0.02	0.2554
	10.31	0	0	15.84	0	0
	0	0.045	0	0	0.12	0
6	2.81	0.04	0.1124	3.03	0.1	0.303
	3.9	0.035	0.1365	6.32	0.08	0.5056
	4.92	0.03	0.1476	9.37	0.06	0.5622
	6.7	0.025	0.1675	12.77	0.04	0.5108
	8.52	0.02	0.1704	16.54	0.02	0.3308
	10.7	0.01	0.107	18.9	0	0
	12.36	0	0			
	0	0.06	0	0	0.16	0
7	4.5	0.05	0.225	3.52	0.14	0.4928
	5.97	0.04	0.2388	6.11	0.12	0.7332
	9.35	0.03	0.2805	8.53	0.1	0.853
	11.55	0.02	0.231	11.46	0.08	0.9168
	13.14	0.01	0.1314	13.77	0.06	0.8262
	14.52	0	0	17.81	0.04	0.7124
				20.02	0.02	0.4004
				22.09	0	0
8	0	0.08	0	0	0.2	0
	4.02	0.07	0.2814	3.54	0.18	0.6372
	5.17	0.06	0.3102	7.04	0.15	1.056
	7.76	0.05	0.388	11.06	0.12	1.3272
	10.53	0.04	0.4212	14.13	0.09	1.2717
	12.46	0.03	0.3738	18.82	0.06	1.1292
	14.02	0.02	0.2804	22.57	0.03	0.6771
	16.61	0	0	25.16	0	0

The plot of the results on Table 4.2 are graphically shown in Figure 4.11, Figure 4.12, Figure 4.13, and Figure 4.14. In Figure 4.11 and Figure 4.12, the VAWT is operated under loading conditions. It can be observed that the higher the external torque is applied, the lower the angular speeds of the VAWT as usual. However, the torques of the VAWT with the wind booster in Figure 4.12 can be exerted at much higher comparatively. It can be interpreted that the VAWT with the wind booster is capable of generate higher mechanical powers as shown in Figure 4.13 and Fig. 4.14. Obviously, the mechanical power of the VAWT with the wind booster is increased in terms of the peak. Also, the operating range of the angular speed of the VAWT is significantly expanded compared with the VAWT without the wind booster.

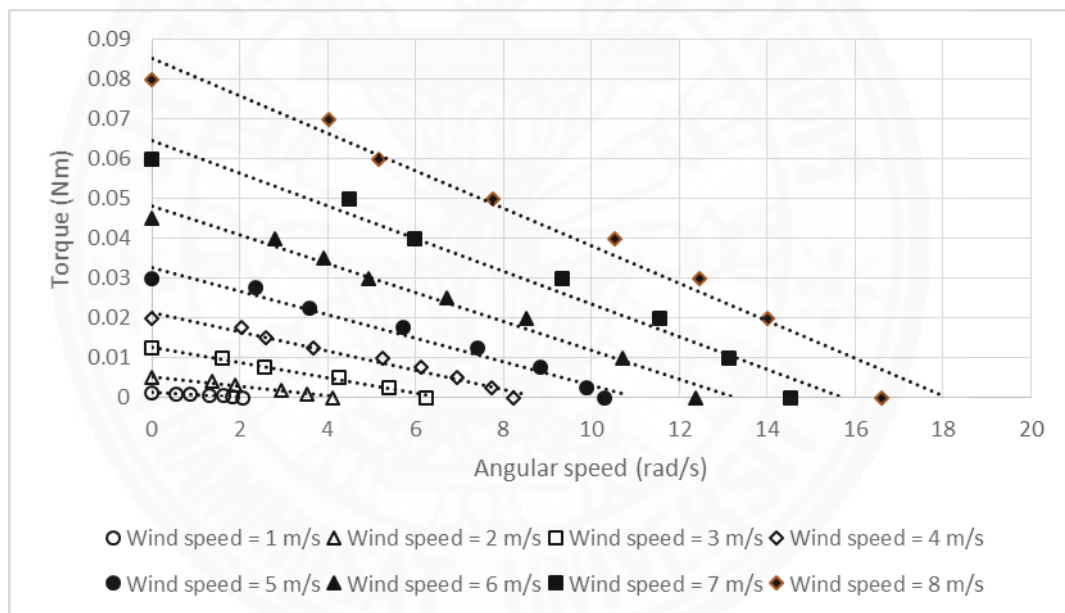


Figure 4.11 Plots of torques against VAWT angular speeds without wind booster

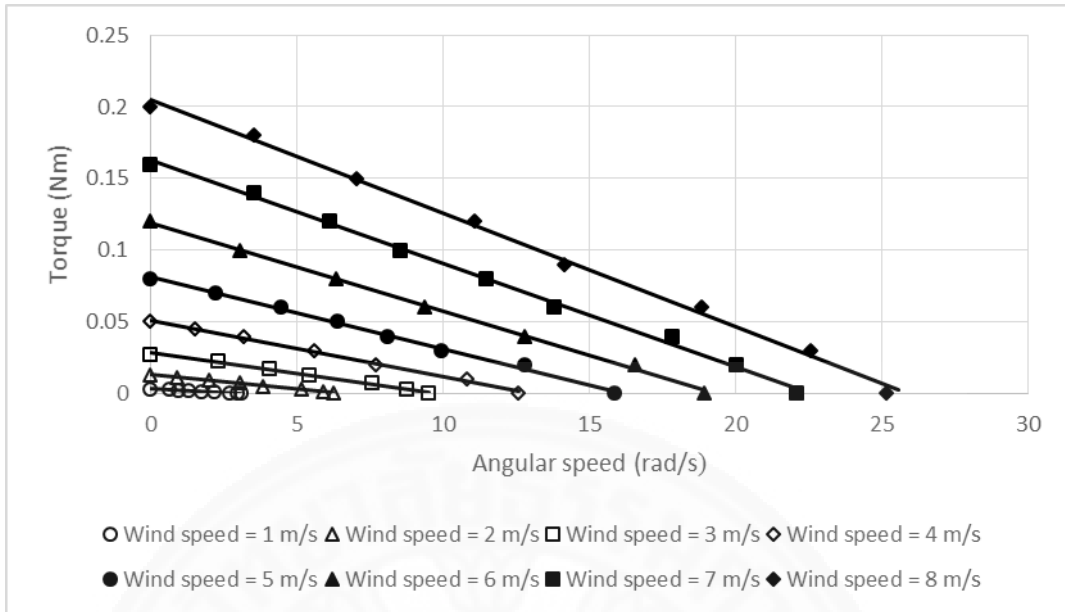


Figure 4.12 Plots of torques against VAWT angular speeds with wind booster

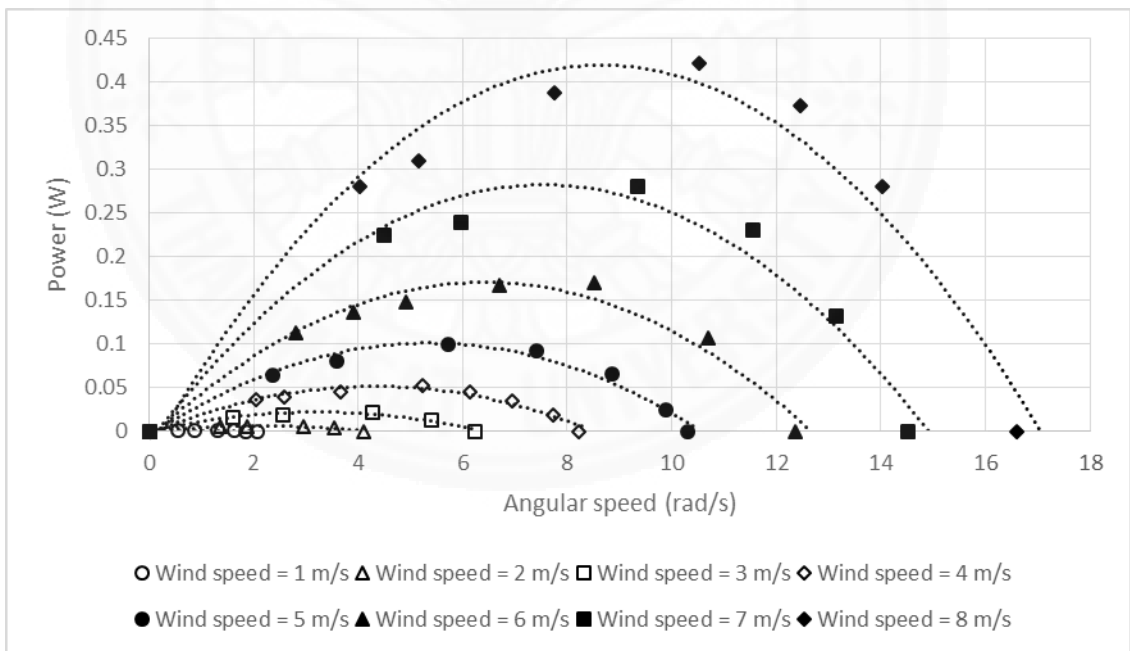


Figure 4.13 Plots of powers against VAWT angular speeds without wind booster



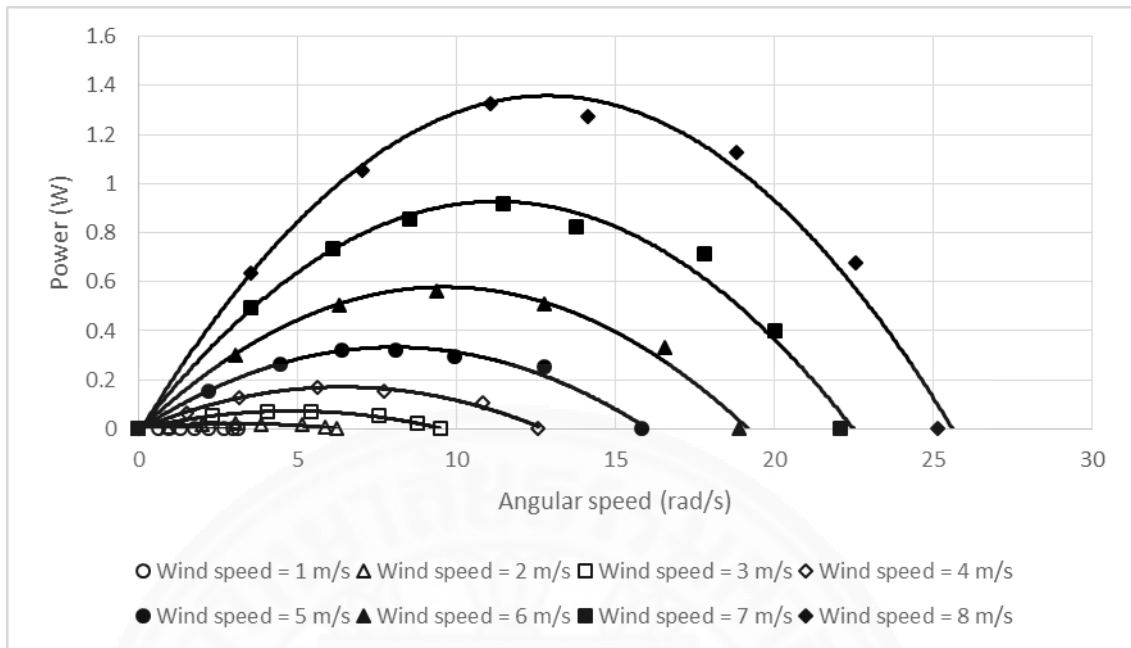


Fig. 4.14 Plots of powers against VAWT angular speeds with wind booster

Accordingly, the plots of the coefficient of power versus tip speed ratio are graphically shown in Figure 4.15. The curve of the coefficient of power in the case of the VAWT with the wind booster significantly shifts over the curve of coefficient of power in the case of the VAWT without the wind booster. Those results means the wind booster improves the efficiency of the VAWT. It can be observed that the characteristic curve is similar whereas the peak value of the coefficient of power is notably higher. The operating range of tip speed ratio of the VAWT is significantly larger. The preliminary design of wind booster is able to greatly increase peak coefficient of power from about 1.4% to 4.5%. However, the wind booster is capable of shifting up to the highest curve of coefficient of power with selecting optimal design variables: number, shape, and leading angle of the guide vane.

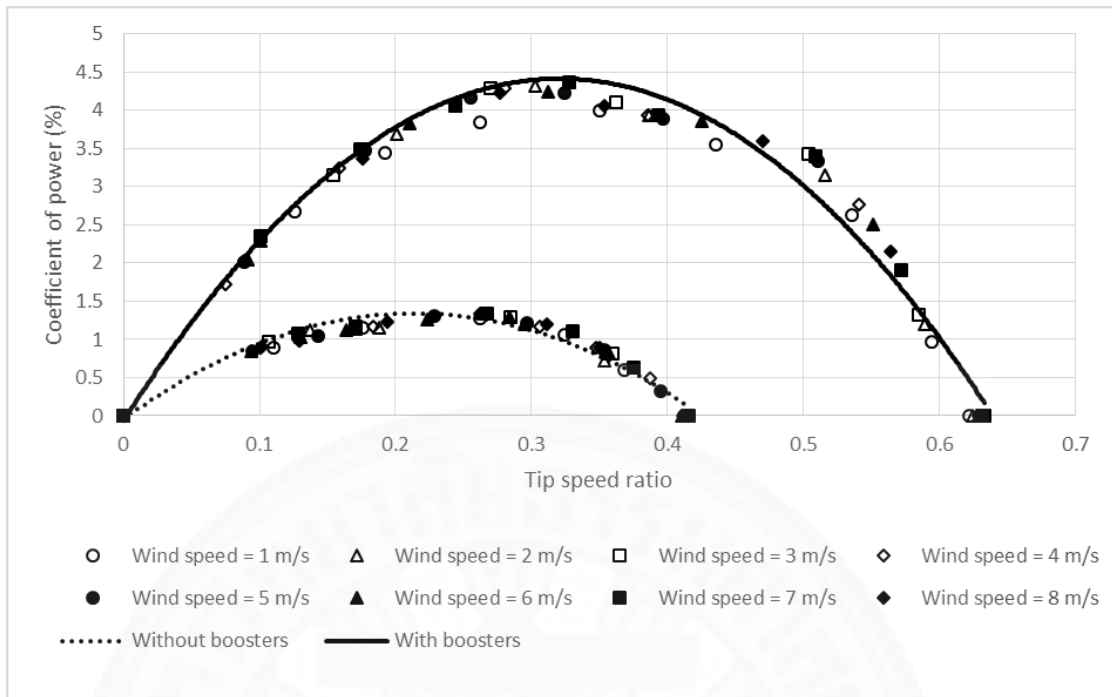


Figure 4.15 Plots of power coefficient against VAWT tip speed ratio

## 4.2 Optimization of wind boosters

In the optimization of the wind booster, the aim is to maximize the peak value of the coefficient of power, which represents the highest ability to convert wind power into mechanical power of VAWTs. It should be noted that both overall value of the coefficient of power and the operating range of tip speed ratio enhance as the peak value of the coefficient of power increases. For each shape, the initial number ( $\beta$ ) and the leading angle ( $\alpha$ ) are set to 6 and  $40^\circ$ , respectively. The initial magnitudes of step for number ( $\delta_\beta$ ) and leading angle ( $\delta_\alpha$ ) of the guide vane are 1 and 5 degree, respectively. However, the magnitude of step for number of the guide vane remains constant all iterations while the leading angle of the guide vane decreases as the optimal solution is approached. The results of the optimization for curved-side-triangle, straight-side-triangle, and straight line guide vanes are listed in Table 4.3, Table 4.4, and Table 4.5 respectively. Figure 4.16 shows the development of the peak value of the coefficient of power for three shapes of the guide vane in each iteration of the proposed technique. The conclusions of optimal design variables are reported in Table 4.6. The straight line shape yields the maximum peak value of the coefficient of power with 6 guide vanes

and leading angle of  $76.1^\circ$ . The advantage of this optimal design with 6 guide vanes and the leading angle of  $76.1^\circ$  is to increase the width of the passages to be able to capture larger amount of inlet wind than the original design with 8 guide vane and leading angle of  $60^\circ$  of the proposed wind booster as illustrated in Figure 3.4. In practice, the guide vane with straight line type is easily fabricated as well.

Table 4.3 Optimization for curved side triangle shape of guide vane

Iteration	$\delta_\beta$	$\delta_\alpha$ ( $^\circ$ )	$\beta$	$\alpha$ ( $^\circ$ )	$\hat{C}_p$ (%)
1	1	5	6	40	2.63
2	1	5	5	40	1.19
3	1	5	7	40	3.06
4	1	5	7	35	2.66
5	1	5	7	45	3.07
6	1	5	8	50	4.44
7	1	5	9	60	2.61
8	1	5	7	50	3.11
9	1	5	9	50	2.59
10	1	5	8	45	4.32
11	1	5	8	55	4.80
12	1	5	8	60	4.38
13	1	5	7	55	4.38
14	1	5	9	55	3.38
15	-	1	8	54	4.75
16	-	1	8	56	4.78
17	-	0.1	8	54.9	4.79
18	-	0.1	8	55.1	4.80
19	-	0.01	8	54.99	4.80
20	-	0.01	8	55.01	4.80

Table 4.4 Optimization for straight side triangle shape of guide vane

Iteration	$\delta_\beta$	$\delta_\alpha$ (°)	$\beta$	$\alpha$ (°)	$\widehat{C}_p$ (%)
1	1	5	6	40	0.34
2	1	5	5	40	2.36
3	1	5	7	40	2.92
4	1	5	7	35	2.57
5	1	5	7	45	3.16
6	1	5	8	50	5.03
7	1	5	9	60	2.72
8	1	5	7	50	3.36
9	1	5	9	50	3.09
10	1	5	8	45	4.86
11	1	5	8	55	5.11
12	1	5	8	60	4.53
13	1	5	7	55	3.53
14	1	5	9	55	2.91
15	-	1	8	54	5.08
16	-	1	8	56	5.00
17	-	0.1	8	54.9	5.13
18	-	0.1	8	55.1	5.10
19	-	0.1	8	54.8	5.13
20	-	0.1	8	54.6	5.14
21	-	0.1	8	54.3	5.10
22	-	0.1	8	54.5	5.13
23	-	0.1	8	54.7	5.14
24	-	0.01	8	54.59	5.14
25	-	0.01	8	54.61	5.14

Table 4.5 Optimization for straight line shape of guide vane

Iteration	$\delta_\beta$	$\delta_\alpha$ (°)	$\beta$	$\alpha$ (°)	$\widehat{C}_p$ (%)
1	1	5	6	40	1.64
2	1	5	5	40	1.46
3	1	5	7	40	0.51
4	1	5	6	35	1.68
5	1	5	6	45	1.71
6	1	5	6	50	1.79
7	1	5	6	60	3.78
8	1	5	6	75	5.25
9	1	5	6	80	5.24
10	1	5	5	75	5.05
11	1	5	7	75	4.89
12	1	5	6	70	4.82
13	1	5	6	80	5.24
14	-	1	6	74	5.34
15	-	1	6	76	5.54
16	-	1	6	77	5.46
17	-	1	5	76	4.88
18	-	1	7	76	4.87
19	-	0.1	6	75.9	5.51
20	-	0.1	6	76.1	5.56
21	-	0.1	6	76.2	5.56
22	-	0.01	6	76.09	5.56
23	-	0.01	6	76.11	5.56

Table 4.6 Optimal design variables for the three different shapes of guide vanes

Shape of guide vanes	Number	Leading angle (°)	$\widehat{C}_p$ (%)
Curved side triangle	8	55	4.80
Straight side triangle	8	54.6	5.14
Straight line	6	76.1	5.56

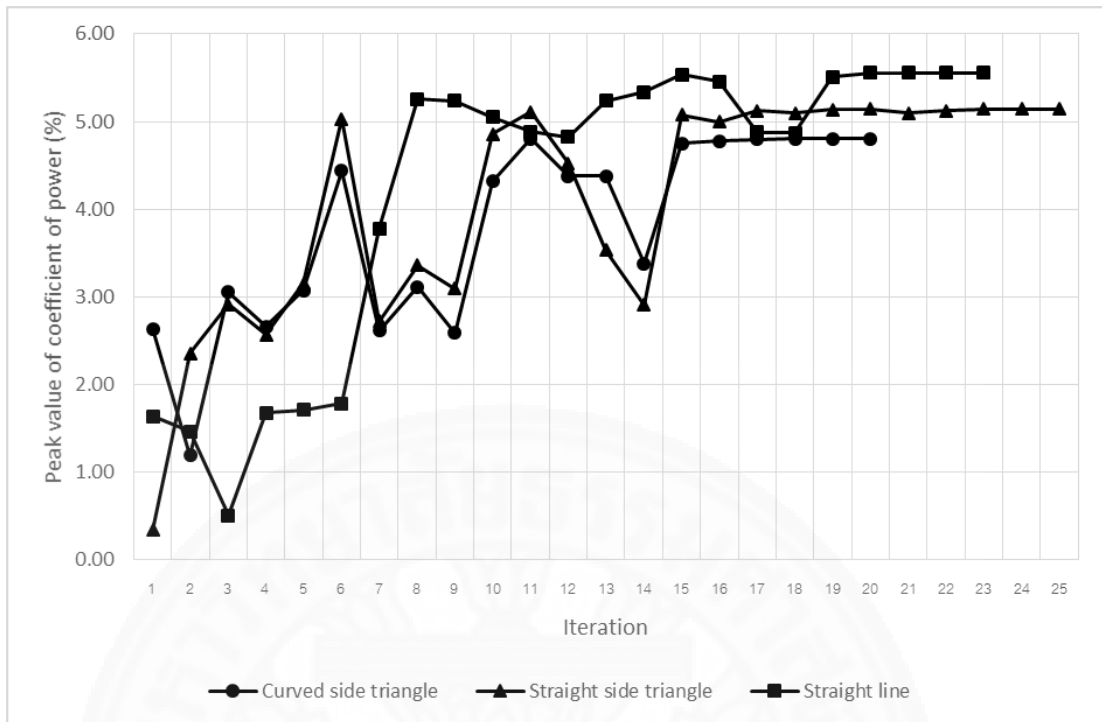


Figure 4.16 Plots of development of peak values of coefficient of power

The optimal design of the wind booster is illustrated in Figure 4.17. The wind booster with straight line shape of guide vanes yields the maximum peak value of the coefficient of power at 5.56 % with 6 guide vanes and leading angle of 76.1°.

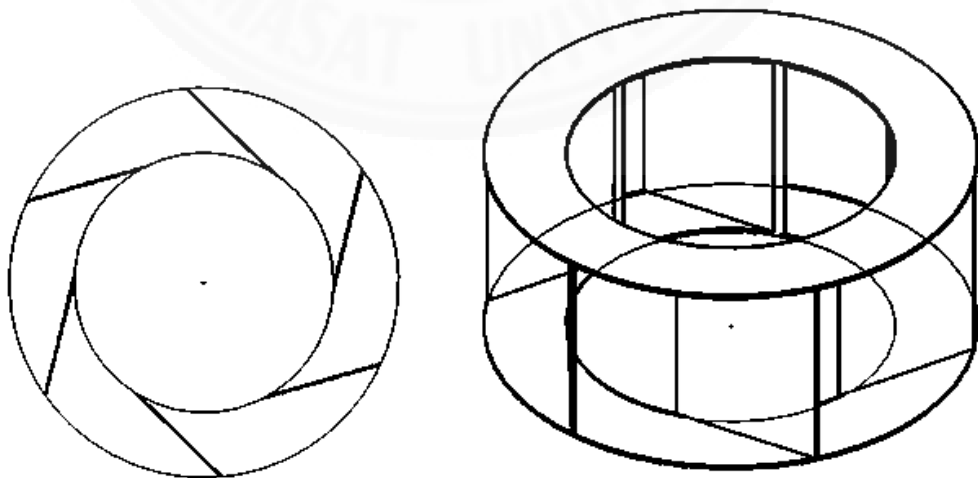


Figure 4.17 The optimal wind booster

It can be noticed that the optimal number of guide vane for curved-side-triangle guide vanes and straight-side-triangle guide vanes are eight while the optimal wind boosters with straight-line guide vanes has six number of guide vane. To ensure the reliability of the optimization approach, the optimization of the wind booster with straight line shape of guide vanes has been repeated by changing the initial value of the number of guide vanes ( $\beta$ ) to 8. The results on Table 4.7 show that even the initial value of the number of guide vanes is changed, the optimal number of guide vanes is still six. Also, the optimal leading angle of guide vanes is still  $76.1^\circ$

Table 4.7 Optimization for straight line shape of guide vane with initial  $\beta$  of 8

Iteration	$\delta_\beta$	$\delta_\alpha$ ( $^\circ$ )	$\beta$	$\alpha$ ( $^\circ$ )	$\widehat{C}_p$ (%)
1	1	5	8	40	0.47
2	1	5	7	40	0.51
3	1	5	9	40	0.34
4	1	5	7	35	0.92
5	1	5	7	45	1.23
6	1	5	7	50	1.55
7	1	5	7	60	3.68
8	1	5	7	75	4.89
9	1	5	7	80	4.64
10	1	5	6	75	5.25
11	1	5	8	75	4.82
12	1	5	6	70	4.82
13	1	5	6	80	5.24
14	-	1	6	74	5.34
15	-	1	6	76	5.54
16	-	1	6	77	5.46
17	-	1	5	76	4.88
18	-	1	7	76	4.87
19	-	0.1	6	75.9	5.51
20	-	0.1	6	76.1	5.56
21	-	0.1	6	76.2	5.56

---

22	-	0.01	6	76.09	5.56
23	-	0.01	6	76.11	5.56

---





## **Chapter 5**

### **Conclusions and Recommendations**

#### **5.1 Conclusions**

The CFD experiments show that the specially-designed wind booster is able to improve mechanical performances of the VAWT at low speed wind conditions. The main mechanism of a wind booster can be separated into 2 functions. The former is “guiding”; the guide vanes direct wind to impact VAWT blades at effective angles. The latter is “throttling”; the passage between each guide vane is set up to throttle air flow to be accelerated before impacting VAWT blades. It can be observed in CFD experiments that the VAWT can rotate faster when it is equipped with a wind booster with 50% of increment on VAWT angular speed in no loading condition. Also, it can produce higher mechanical power in accordance with the experiment under various loading condition, the wind booster is able to greatly increase peak coefficient of power from about 1.4% to 4.5%. The wind booster additionally tested under fluctuating-speed wind and it performed well even in extremely weak wind condition. With optimization technique, the optimal design of wind booster is found. the VAWT with optimal wind booster, which consists of 8 straight-line guide vanes and leading angle of  $76.1^\circ$ , is capable of producing mechanical power higher up to the coefficient of power of 5.56 % than the original design. The proposed methodology helps to overcome the limitation of very low power in low speed wind, particularly, taking place in Thailand.

#### **5.2 Recommendations**

Harvesting low availability of energy from low speed wind seems to be impossible in the past but thanks to improvement of wind technology, waste energy is not waste anymore. The study of wind booster is the one of the wind technology that make an effort to overcome this limitation and the great results are found. However, there might be another new approach which can improve energy harvesting form low speed wind. The VAWT or even another type of wind turbine could be specifically design to better suit with low speed wind. Combination of a good low speed wind turbine and a wind booster should be able to improve energy harvesting for low speed

wind even higher. For future work, there is a concept idea to integrate VAWT with another type of renewable energy-based device in order to improve capability to generate power from multiple energy resource. For example, wind solar hybrid system, VAWT with wind booster could be designed to capture the solar energy by coupling with the solar cell system which should be sufficient to perpetually generate electricity for a small light bulb.



## References

### Books and Book Articles

- Akwa, J.V., Vielmo, H.A., Petry, A.P. (2012). A review on the performance of Savonius wind turbines. *Renewable and Sustainable Energy Reviews*, 16, 3054-3064.
- Ali, M.H. (2013) Experimental comparison study for Savonius wind turbine of two & three blades at low wind speed. *International Journal of Modern Engineering Research*, 3(5), 2978-2986.
- Chong, W.T., Poh, S.C., Fazlizan, A., Pan, K.C. (2012). Vertical axis wind turbine with Omni-directional-guide-vane for urban high-rise building. *Journal of Central South University*, 19, 727–732.
- Korprasertsak, N., Korprasertsak, N. and Leephakpreeda, T. (2014). CFD modeling and design of wind Boosters for low speed vertical axis wind turbines. *Proceedings of the 5<sup>th</sup> International Conference on Mechanical and Aerospace Engineering July 18-19, 2014 (pp.5)*, Madrid, Spain.
- Korprasertsak, N., Korprasertsak, N. and Leephakpreeda, T. (2014). CFD modeling and design of wind Boosters for low speed vertical axis wind turbines. *Advanced Materials Research*, 1016, 554-558
- Leephakpreeda, T. (2000). *Optimization: principle and algorithm*. Bangkok, Thailand: Thammasat Press.
- Major, S., Commins, T., Nopparatana, A. (2008). Potential of wind power for Thailand: an assessment. *Maejo International Journal of Science and Technology*, 2(2), 255-266.
- Ohya, Y., Karasudani, T. (2010). A shrouded wind turbine generating high output power with Wind-lens technology. *Energies*, 3(4), 634-649.
- Pope, K., Rodrigues, V., Doyle, R., Tsopelas, A., Gravelins, R., Naterer, G.F., Tsang, E. (2010). Effects of stator vanes on power coefficients of a Zephyr vertical axis wind turbin. *Renewable Energy*, 35, 1043–1051.
- Takao, M., Kuma, H., Maeda, T., Kamada, Y., Oki, M., Minoda, A. (2009). A Straight-Bladed vertical axis wind turbine with a directed guide vane row- effect of guide vane geometry on the performance. *Journal of Thermal Science*, 18(2), 54-57.

Walker, J.A. (2009). Wind power – a firm foundation for a century of renewable energy growth. *IOP Conf. Series: Earth and Environmental Science* 6, IOP Publishing.

Wang, S., Ingham, D.B., Ma, L., Pourkashanian, M., Tao, Z. (2010). Numerical investigations on dynamic stall of low Reynolds number flow around oscillating airfoils. *Comput. Fluids*, 39, 1529–1541.

### **Electronic Media**

Ministry of Energy. (2013). *Thailand Wind Map*. Retrieved from September 29, 2013, <http://www2.dede.go.th/report/E6-3.pdf>

Musavi, S.H., Ashrafizaadeh, M. (2015). Meshless lattice Boltzmann method for the simulation of fluid flows. *Physical Review E*, 91 Retrieved from March 14, 2015, <http://journals.aps.org/pre/abstract/10.1103/PhysRevE.91.023310>

Next Limit Technologies. (2015). *XFlow 2014- computational fluid dynamics*.

Retrieved from April 20, 2015,

[http://www.xflowcf.com/pdf/Product\\_sheet\\_2014.pdf](http://www.xflowcf.com/pdf/Product_sheet_2014.pdf)



**Appendices**

## Appendix A

### Estimation of Peak Coefficient of Power

When plotting the graph of torques against VAWT angular speed, the torque can be estimated by the linear equation shown below:

$$T = -\frac{T_{max}}{\omega_{max}}\omega + T_{max} \quad (A.1)$$

where  $T_{max}$  is the maximum torque which allows the VAWT rotation (Nm), and  $\omega_{max}$  is the VAWT angular speed at no load (rad/s).

By multiplying the VAWT angular speed to (A.1), the VAWT power output can be expressed by the square polynomial equation shown below:

$$P_T = -\frac{T_{max}}{\omega_{max}}\omega^2 + T_{max}\omega \quad (A.2)$$

To determine the peak VAWT power output, let  $\frac{\partial P_T}{\partial \omega} = 0$ . Therefore, the peak VAWT power output occurs where  $\omega = \frac{1}{2}\omega_{max}$ . It can be expressed as:

$$\hat{P}_T = \frac{1}{4}T_{max}\omega_{max} \quad (A.3)$$

where  $\hat{P}_T$  is the peak power output (W).

Hence the peak power coefficient can be expressed as:

$$\hat{C}_p = \frac{1}{4} \frac{T_{max}\omega_{max}}{P} \quad (A.4)$$

where  $\hat{C}_p$  is the peak coefficient of power

## Appendix B

### VAWT Angular speed VS time

From Figure B.1 to Figure B.8, the raw results of VAWT angular speed against time in no loading condition for wind speed of 1-8 m/s are shown respectively. The VAWT rotation starts from the transient state until the rotation becomes steady. The steady state of the VAWT rotation can be notice where the VAWT angular speed nearly remains constant. Also, the results shows the capability of wind booster that shifts up the VAWT angular speed in steady state.

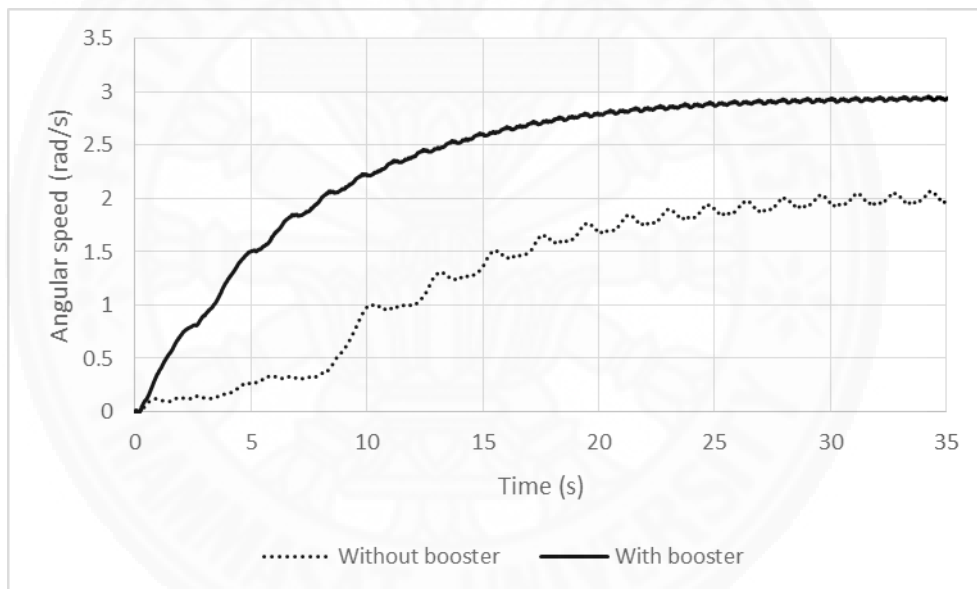


Figure B.1 Plot of VAWT angular speed against time for wind speed of 1 m/s

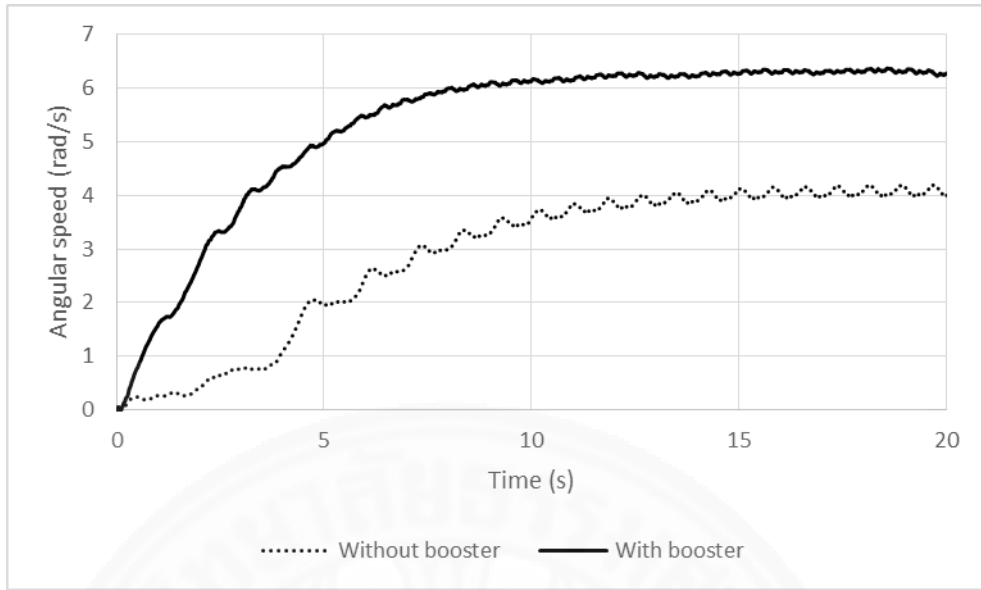


Figure B.2 Plot of VAWT angular speed against time for wind speed of 2 m/s

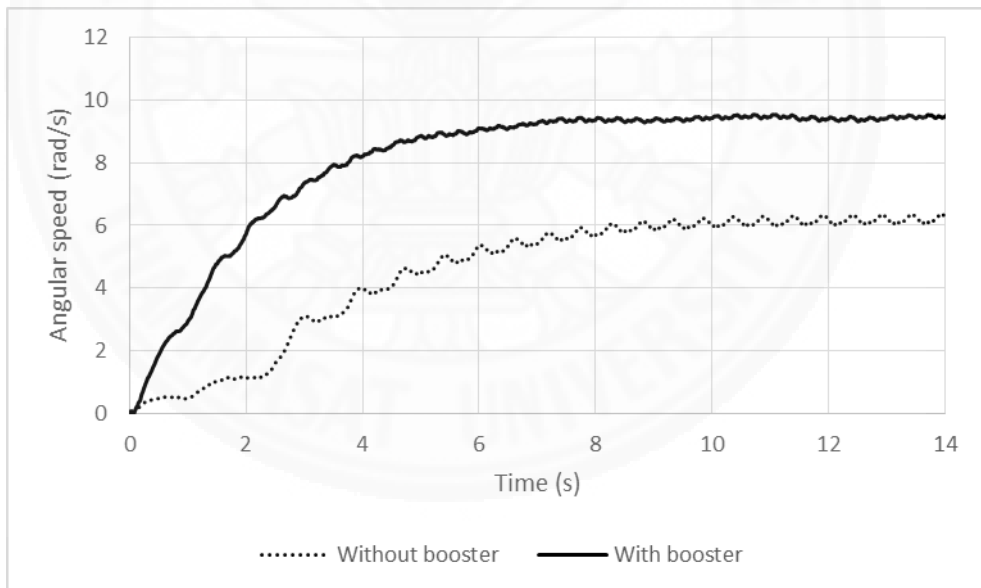


Figure B.3 Plot of VAWT angular speed against time for wind speed of 3 m/s



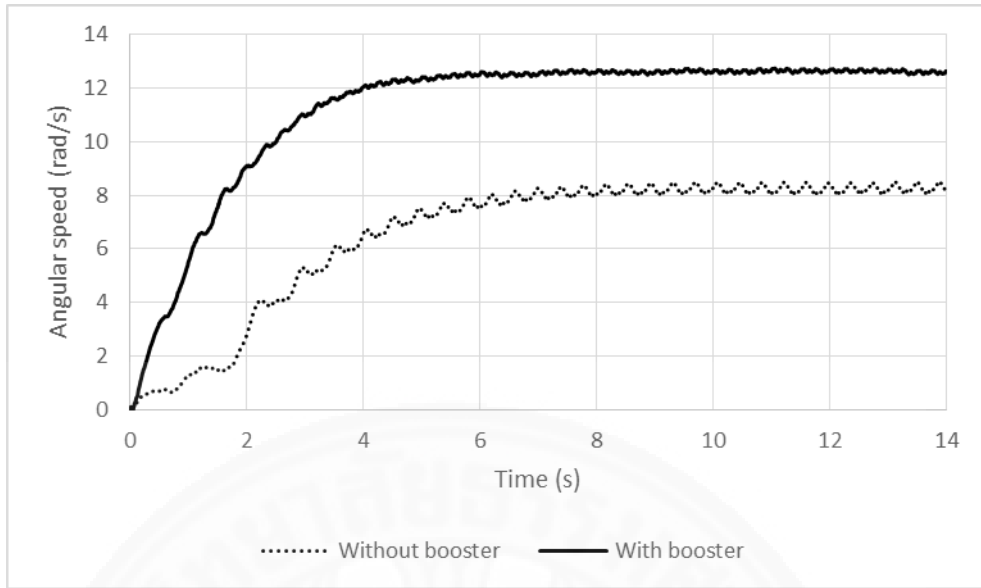


Figure B.4 Plot of VAWT angular speed against time for wind speed of 4 m/s

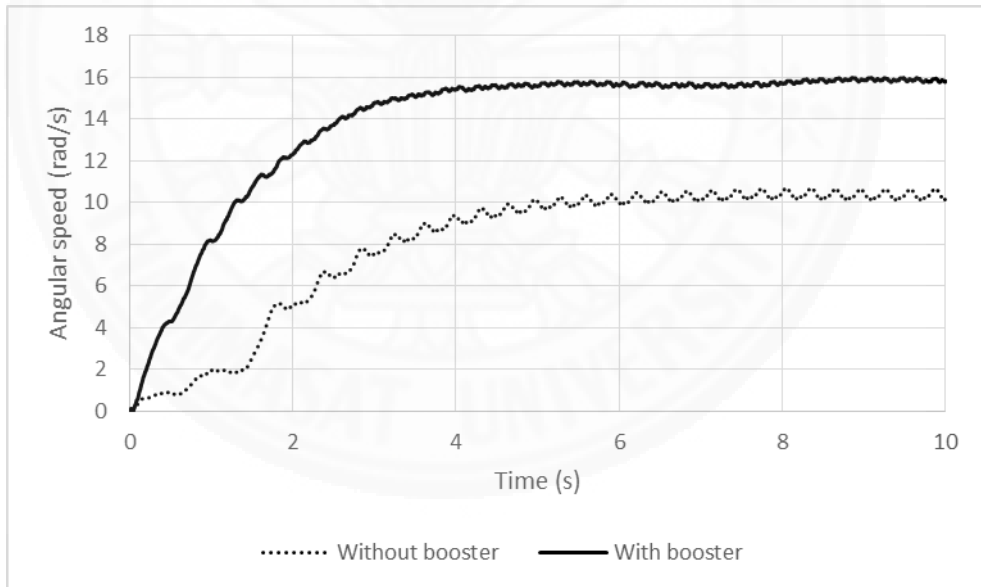


Figure B.5 Plot of VAWT angular speed against time for wind speed of 5 m/s

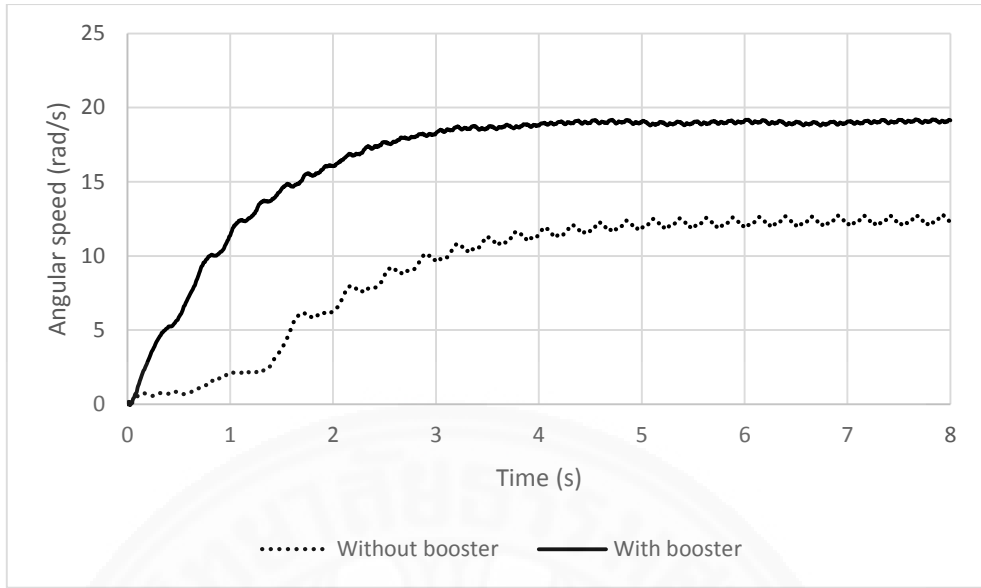


Figure B.6 Plot of VAWT angular speed against time for wind speed of 6 m/s

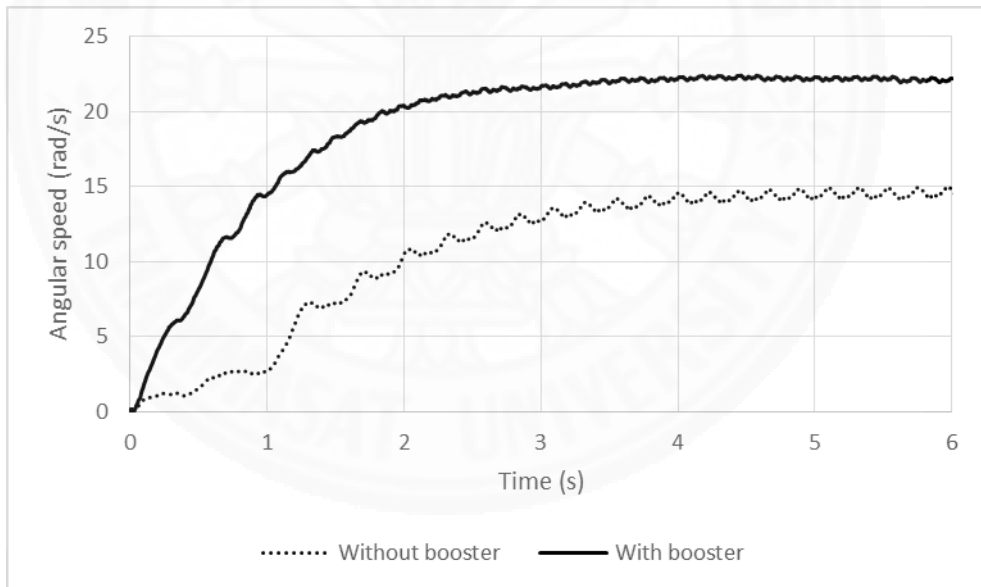


Figure B.7 Plot of VAWT angular speed against time for wind speed of 7 m/s

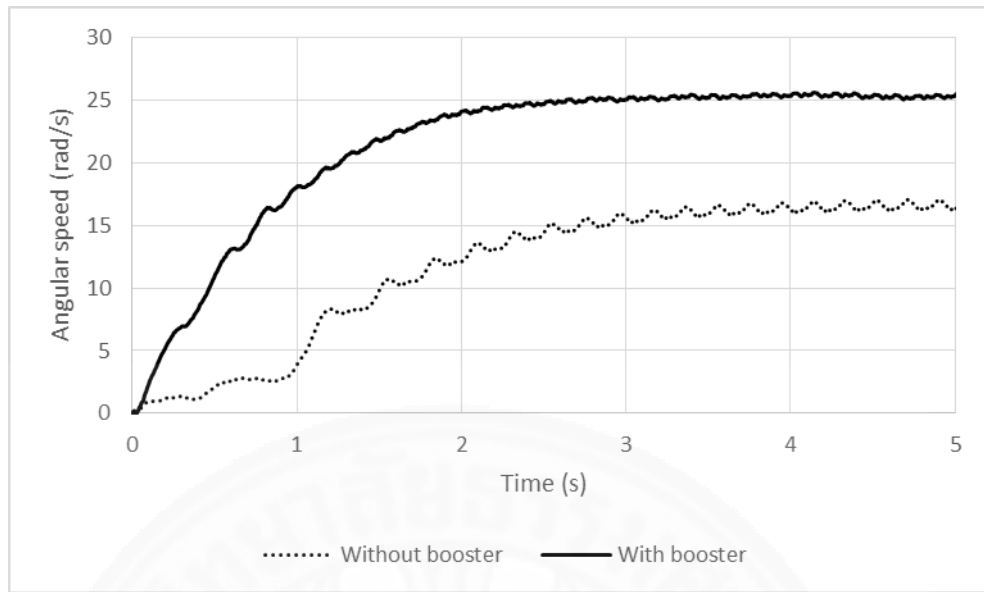


Figure B.8 Plot of VAWT angular speed against time for wind speed of 8 m/s